research articles Journal of proteome •research

Glycomic Analysis of Alpha-Fetoprotein L3 in Hepatoma Cell Lines and Hepatocellular Carcinoma Patients

Takatoshi Nakagawa,[¶] Eiji Miyoshi,[‡] Takayuki Yakushijin,[§] Naoki Hiramatsu,[§] Takumi Igura,[§] Norio Hayashi,[§] Naoyuki Taniguchi,[†] and Akihiro Kondo*,[¶]

Department of Glycotherapeutics, Department of Functional Diagnostic Science, Division of Health Science, Department of Gastroenterology and Hepatology, Osaka University Graduate School of Medicine, 2-2 Yamadaoka, Osaka 565-0871, Japan and Department of Disease Glycomics, Research Institute for Microbial Diseases, Osaka University, 3-1 Yamadaoka, Suita, Osaka 565-0871, Japan

Received September 21, 2007

The *N*-glycan structures of the *Lens culinaris* agglutinin (LCA)-reactive fraction of alpha-fetoprotein (AFP-L3), a tumor marker of hepatocellular carcinomas (HCC), were analyzed in relationship to glycosyltransferases and LCA-affinity electrophoresis. Using HPLC and MALDI-TOF MS, we determined the *N*-glycan structures of AFP from HCC cell lines, and demonstrated they were affected by *N*-acetylglucosaminyltransferase III and fucosyltransferase VIII, but not by *N*-acetylglucosaminyltransferase V. Moreover, we identified the *N*-glycan structures of AFP in HCC patients.

Keywords: AFP-L3 • core-fucosylation • glycosyltransferase • hepatocellular carcinoma • LCA-affinity electrophoresis • *N*-glycan • tumor marker

Introduction

Alpha-fetoprotein (AFP) is an oncofetal glycoprotein that contains a single glycosylation site at the level of asparagine 232, and is a well-known tumor marker for hepatocellular carcinomas (HCC). [1] However, the AFP concentration is also elevated in other liver diseases, such as chronic hepatitis and cirrhosis.[2] Recently, the *Lens culinaris* agglutinin (LCA)-reactive fraction of AFP (AFP-L3) has been measured as a more specific marker for HCC. AFP-L3 reflects HCC-specific changes in the glycans of AFP.[3] AFP-L3 exhibits superior specificity and sensitivity compared with the total AFP concentration.[4,5] Also, AFP-L3 is strongly correlated with the HCC patient outcome: a high level of AFP-L3 is indicative of a poor patient prognosis.[6,7]

AFP-L3-positive patients exhibit pathological features that are characteristic of a HCC that has progressed.[8] The activity of α-1,6 fucosyltransferase (fucosyltransferase VIII; FUT8) has been implicated in the production of AFP-L3. FUT8 catalyzes the transfer of fucose to the proximal GlcNAc of an *N*-glycan via an α1,6 linkage—a process known as "core-fucosylation."[9]

A variety of glycosyltransferases are involved in the formation of complex and hybrid types of *N*-glycans. The glycan structures examined in this report, the corresponding glycosyltransferases, and the biosynthetic pathway of complex *N*-glycan are summarized in Table 1. In this biosynthetic pathway, *N*-acetylglucosaminyltransferase I (GnT-I) triggers a series of reactions involving the addition of a GlcNAc via a β1,2-linkage in a mannose (Man) α1,3 Man- structure. Subsequently, GnT-II transfers a GlcNAc to a Manα1,6 Man-structure via a β1,2-linkage. Among the *N*-glycans examined in this study, GnT-I and -II are involved in the synthesis of all the *N*-glycans and all the *N*-glycans except for GnF, respectively (Table 1, lower panel). Furthermore, other glycosyltransferases, that is, GnT-III, GnT-IV, GnTV, and FUT-8, participate in the formation of complex-type *N*-glycans (Table 1, upper panel). GnT-IV and GnT-V catalyze the addition of GlcNAc to GlcNAcβ1,2Manα1,6Manβ-R via a β1,4-linkage, and GlcNAcβ1,2Manα1,6Manβ-R via a β1,6-linkage, respectively. G2GF-tri and G2G-tri glycans, and GG2-tri and GG2F-tri glycans in this study involve GnT-V and GnT-IV, respectively (Table 1, lower panel). GnT-III transfers a GlcNAc at a Manβ1,4GlcNAcβ-structure via a β1,4-linkage, the so-called "bisecting GlcNAc". G2(Gn)F-bi glycan is a GnT-III product here (Table 1, lower panel). It is noteworthy that a bisecting GlcNAc inhibits the actions of GnT-IV and -V. In other words, GnT-III is a key determinant of complex-type *N*-glycan structures. As mentioned above, FUT8 is responsible for core-fucosylation and involved in the synthesis of GnF, G2F-bi, GG2F-tri, G2(Gn)F-bi, and G2GF-tri glycans (Table 1, lower panel).

AFP has one *N*-glycan, but its structure varies with the developmental stage and disease state. AFP in ascites fluid from an HCC patient contained primarily biantennary glycans with a core-fucose, in addition to glycans exhibiting various degrees of sialylation.[10] In contrast, yolk sac tumors secrete AFP with a bisecting GlcNAc.[11] During fetal development, core-fucosylated glycans are at a high level at an early stage and then decrease throughout gestation.[12] Glycan analysis demonstrated that human cord serum contains core-fucosylated and non-

* To whom correspondence should be addressed. E-mail: kondoa@glycot.med.osaka-u.ac.jp. Tel.: 81-6-6879-3648. Fax: 81-6-6879-3646.

[¶] Department of Glycotherapeutics, Osaka University Graduate School of Medicine.

[‡] Department of Functional Diagnostic Science, Osaka University Graduate School of Medicine.

[§] Department of Gastroenterology and Hepatology, Osaka University Graduate School of Medicine.

[†] Department of Disease Glycomics, Osaka University.

Published on Web 05/15/2008

10.1021/pr700841q CCC: $40.75

Table 1. Biosynthetic Pathway and Summary of *N*-Glycans Examined in This Study[a]

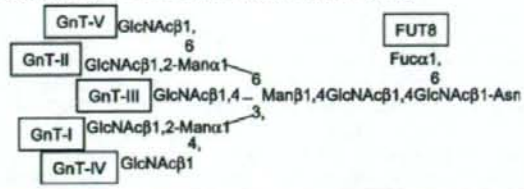

Structures	Symbols[a]	Enzymes[b]
Fucα1, 6 Manα1, 6 GlcNAcβ1,2-Manα1,3 Manβ1,4GlcNAcβ1,4GlcNAc	GnF	GnT-I, **FUT8**
Galβ1,4GlcNAcβ1,2-Manα1, 6 Galβ1,4GlcNAcβ1,2-Manα1, 3 Manβ1,4GlcNAcβ1,4GlcNAc	G2-bi	GnT-I, GnT-II
Fucα1, 6 Galβ1,4GlcNAcβ1,2-Manα1, 6 Galβ1,4GlcNAcβ1,2-Manα1, 3 Manβ1,4GlcNAcβ1,4GlcNAc	G2F-bi	GnT-I, GnT-II **FUT8**
Galβ1,4GlcNAcβ1,2-Manα1, 6 Galβ1,4GlcNAcβ1,2-Manα1, 3 Manβ1,4GlcNAcβ1,4GlcNAc 4, Galβ1,4GlcNAcβ1	GG2-tri	GnT-I, GnT-II GnT-IV
Fucα1, 6 Galβ1,4GlcNAcβ1,2-Manα1, 6 Galβ1,4GlcNAcβ1,2-Manα1, 3 Manβ1,4GlcNAcβ1,4GlcNAc 4, Galβ1,4GlcNAcβ1	GG2F-tri	GnT-I, GnT-II GnT-IV, **FUT8**
Fucα1, 6 Galβ1,4GlcNAcβ1,2-Manα1, 6 GlcNAcβ1,4 Manβ1,4GlcNAcβ1,4GlcNAc Galβ1,4GlcNAcβ1,2-Manα1, 3	G2(Gn)F-bi	GnT-I,GnT-II **GnT-III, FUT8**
Galβ1,4GlcNAcβ1, 6 Fucα1, 6 Galβ1,4GlcNAcβ1,2-Manα1, 6 Galβ1,4GlcNAcβ1,2-Manα1, 3 Manβ1,4GlcNAcβ1,4GlcNAc	G2GF-tri	GnT-I,GnT-II **GnT-V, FUT8**
Galβ1,4GlcNAcβ1, 6 Galβ1,4GlcNAcβ1,2-Manα1, 6 Galβ1,4GlcNAcβ1,2-Manα1, 3 Manβ1,4GlcNAcβ1,4GlcNAc	G2G-tri	GnT-I,GnT-II **GnT-V**

[a] GnT-I, II, III, IV, and V, *N*-acetylglucosaminyltransferase I, II, III, IV, and V; FUT8, fucosyltransferase VIII; GlcNAc, *N*-acetylglucosamine; Man, mannose; Fuc, fucose; Asn, asparagine. a: the symbol for each *N*-glycan examined in this study. b, major glycosyltransferases involved in the formation of each *N*-glycan. The glycosyltransferases in red were focused on in this study.

core-fucosylated biantennary glycans. Noncore-fucosylated glycans were 19 times more abundant than core-fucosylated ones. Therefore, fucosylation of AFP has been implicated in the dedifferentiation of hepatocytes that occurs as a HCC progresses.[12]

AFP-L3 can be measured by LCA affinity electrophoresis together with antibody-affinity blotting.[3] Phytohemagglutinin E_4 (E_4-PHA), a GlcNAc binding lectin, is also used for lectin affinity electrophoresis of AFP. The molecular basis for the different affinities of AFP for LCA and E_4-PHA may be the three structural features of *N*-glycans: core-fucosylation at a proximal *N*-acetylglucosamine (GlcNAc) strengthens LCA binding; sialylation at the nonreducing end weakens E_4-PHA binding; and a bisecting GlcNAc strengthens E_4-PHA binding, but not LCA binding.[3,13-15] However, there have only been a few published reports describing the precise glycan structures of AFP in HCC. Among them, Aoyagi et al. used a combination of lectin chromatography (concanavalin A and LCA) and HPLC/pyridylaminated glycan analysis to identify six types of glycans, revealing different glycan subsets for HCC and gallbladder carcinomas.[16] The *N*-glycans of AFP were divided into four fractions: ConA-/LCA-reactive, ConA-nonreactive/LCA-reactive, ConA-reactive/LCA-nonreactive, and ConA-/LCA-nonreactive. The *N*-glycan structures then were determined for each frac-

tion. This classification is similar to that of AFP-L1 to - L3; however, they do not directly correspond with each other. The Food and Drug Administration (FDA) recently approved a laboratory test for AFP-L3 that facilitates determination of the risk of developing liver cancer. Glycomic analysis of AFP will help us understand the molecular basis and clinical meaning of AFP-L3.

Glycan structures are controlled through sequential reactions of various glycosyltransferases within the Golgi apparatus. In HCC, increased FUT8 activity and elevated levels of core-fucose have been reported in both hepatic tissues and sera.[17] Our group previously reported correlations between glycosyltransferase activities and AFP glycan structures in hepatoma (HepG2 and Huh7) and hepatoblastoma (Huh6) cells.[18] To further examine the relationship between glycan structure and glycosyltransferase activity, especially in relation to LCA-affinity electrophoresis, the glycan structures of AFP expressed by Huh7 cells with altered activities of glycosyltransferases, that is, GnT-III, GnT-V, and FUT8, were determined. These three enzymes play pivotal roles in the *N*-glycan synthesis of glycoproteins. AFP was fractionated using LCA-Sepharose, and glycans derived from LCA-bound AFP (which presumably included AFP-L3 and AFP-L2) were also analyzed. In addition, AFP from HCC patients was carefully analyzed. To focus on the involvement of the core structures of *N*-glycans in the AFP/LCA interaction, terminal sialic acids were omitted from the analysis. The bisecting GlcNAc in biantennary glycans with core-fucose caused by the introduction of GnT-III led to the inversely proportional augmentation of the AFP-L2 level as to AFP-L3. Interestingly, the triantennary structure formed through catalysis by GnT-V had no effect on the LCA-affinity electrophoresis pattern or LCA-binding of AFP, regardless of the presence or absence of core-fucose. In addition, knockdown of *FUT8* was directly mirrored by the decreased core-fucose and decrease in AFP-L3. These results were the same for AFP from HCC patients. The present study demonstrated that the affinities of *N*-glycans to LCA, which are regulated by glycosyltransferases, genuinely determine the pattern of LCA-affinity electrophoresis of AFP from cultured cells and from HCC patients.

Materials and Methods

Cell Culture. Huh7 cells were purchased from the ATCC (Manassas, VA). Huh7 cells and glycosyltransferase transfectants were cultured in Dulbecco's Modified Eagle Medium (DMEM)/10% fetal bovine serum (Biowest, Miami, FL), 100 U/mL ampicillin, and 100 μg/mL streptomycin (Nacalai Tesque, Kyoto, Japan).

AFP from HCC Patients. AFP derived from a mixture of sera and ascites fluids from three and 30 patients, respectively, with HCC, 877A, was kindly provided by Drs. Hiroko Taga and Yasuo Endo.[19] The AFPs from one patient with cholangiocarcinoma and two patients with HCC were obtained from Osaka University Hospital (Suita, Osaka, Japan). The ethics committee of Osaka University Hospital (Suita, Osaka, Japan) approved the study protocol and written informed consent was obtained from each patient.

Establishment of Huh7 Transfectants. Huh7*FUT8*KD cells were established by retroviral introduction of siRNA against *FUT8* as previously described.[20] Cells were selected with 500 μg/mL G418 for 2 weeks. The human GnT-III (hGnT-III) gene was retrovirally introduced into Huh7 cells (Huh7*GnT-III*) and then subcloned into pLHCX (Clontech, Mountain View, CA). The retrovirus was prepared with a Retrovirus Packaging Kit Ampho (Takara Bio, Inc., Shiga, Japan), according to the manufacturer's protocol. The human GnT-V gene was adenovirally introduced into Huh7 cells (Huh7*GnT-V*).

Purification of AFPs. For AFP purification, an anti-AFP antibody (DAKO, Denmark) was conjugated to NHS-activated Sepharose 4B according to the manufacturer's instructions. Cells at 80% confluence were cultured in serum-free DMEM for 3 days to collect conditioned medium, which contained secreted AFPs. The collected medium was applied to the anti-AFP column and then eluted with 0.1% trifluoroacetic acid after extensive washing with PBS. The eluate was evaporated using a Speed-Vac (Labconco, Kansas City, MO). The AFP concentrations were determined by measuring the absorbance at 280 nm using a Nanodrop spectrophotometer (Nanodrop Technologies, Wilmington, DE). The purity of the AFPs was confirmed by SDS-PAGE, in conjunction with CBB staining, as shown in Supporting Information Figure 1.

SDS-PAGE, Western Blotting, and Lectin Blotting. The monoclonal anti-FUT8 -GnT-III and -GnT-V antibodies were described previously.[21–23] The monoclonal anti-AFP antibody was purchased from Sigma-Aldrich (St. Louis, MO). Five micrograms of cellular proteins (for FUT8 detection, 20 μg) was electrophoresed and then blotted onto a PVDF membrane (Immobilon P, Millipore). After blocking with 5% nonfat milk in Tris-buffered saline (TBS, 25 mM Tris, 0.15 M NaCl, pH7.4) for 1 h, the membrane filter was incubated with a 1/1000 dilution of each antibody for an additional hour. The membrane filter was then washed with TBS containing 0.05% Tween 20 (TBS-T), three times for 10 min each, and then the second antibody was added at a dilution of 1/2000. After washing with TBS-T, three times for 10 min each, the membrane was developed with an ECL kit (GE Healthcare UK Ltd., Buckinghamshire, U.K.) according to the manufacturer's protocol. The image was captured using a ChemiDoc imaging system (Bio-Rad, Hercules, CA). Biotin-conjugated E_4-PHA and L_4-PHA (phytohemagglutinin L_4)[24] were obtained from Seikagaku Corp. (Tokyo, Japan). An *Aspergillus oryzae* lectin (AOL), a fucose-binding lectin,[25,26] was purchased from Tokyo Chemical Industry Co., Ltd. (Tokyo, Japan). The AOL was biotinylated using sulfo-NHS-biotin (Pierce, Rockford, IL) according to the manufacturer's protocol. After electroblotting, the membrane was blocked with 5% BSA in TBS for several hours. After washing with TBS-T every 10 min for 40 min, the membrane was incubated with each type of lectin for several hours, and then the bound lectin was detected using an ABC kit (Vector Research Laboratory). ECL (GE Healthcare UK Ltd., U.K.) was used for visualization.

Lectin Affinity Electrophoresis Using LCA. LCA electrophoresis was performed with an AFP-L3 Differentiation Kit L (Wako Pure Chemicals, Osaka, Japan) according to the manufacturer's instructions. Briefly, each AFP was prepared at a concentration of 100 ng/mL in AFP-L3 buffer (Wako Pure Chemicals). A sample (2 μL) was subjected to electrophoresis on an agarose gel containing LCA. The separated AFP was transferred to a membrane, followed by antibody-affinity blotting.

Glycan Analysis. *N*-Glycans were released from AFPs and then labeled with 2-aminopyridine (2-AP) as described previously.[27,28] Purified AFP samples (10–20 μg) were briefly dried using a Speed-Vac (Labconco Corp., Kansas City, MO), and then were carbamidomethylated with 5 mM dithiothreitol and 15 mM iodoacetamide in 10 μL of 0.1% Rapigest (Waters Corp., Milford,

MA). *N*-Glycans were released by overnight incubation with 0.5 mU of glycopeptidase F (PNGase; Takara Bio, Inc., Shiga, Japan) at 37 °C. The glycans were incubated with 50 mM sodium acetate for an additional 30 min, lyophilized, and then labeled with GlycoTag (Takara Bio, Inc.), according to the manufacturer's instructions. Excess 2-AP was removed with a cellulose cartridge glycan preparation kit (Takara Bio, Inc.), and the glycans were incubated with 2 M acetic acid at 80 °C for 2 h to remove sialic acids. Pyridylamino (PA) -glycans derived from AFP were analyzed with a reverse phase HPLC system (Waters Corp., Milford, MA) equipped with a PALPAK type R-MB column (2 mmΦ × 150 mm; Takara Bio, Inc.) at the flow rate of 0.5 mL/min using 10 mM sodium phosphate (pH 4.4) (solvent A) and then the same buffer containing 0.5% 1-butanol (solvent B) at 40 °C. The glycans were separated with a gradient of 0−50% solvent B for 30 min followed by 10 min of 50% solvent B. PA-glycans were detected using a fluorescence detector (Waters 2475) at wavelengths of 320 nm for excitation and 400 nm for emission. Four standard PA-sugars, a biantennary sugar, G2-bi (PA-sugar Chain 001), and a biantennary sugar with core-fucose, G2F-bi (PA-Sugar Chain 009), and a triantennary glycan with and without core-fucose, GG2-tri and GG2F-tri (PA-sugar Chain 002 and 010, respectively), were purchased from Takara Bio, Inc., and bisecting biantennary, G2(Gn)-bi (PA-Oligosaccharide 201.4), and core-fucosylated, bisecting biantennary, G2(Gn)F-bi (PA- Oligosaccharide 211.4) sugar chains were obtained from Seikagaku Corp. These standard PA-sugars were routinely utilized as external controls for determining *N*-glycan structures and for HPLC calibration.

MALDI-TOF MS Analysis. PA-glycans derived from AFPs were mixed with 10 mg/mL super dihydroxybenzoic acid, SDHB (Bruker Daltonics, Germany), in 50% acetonitrile/0.1% TFA. The mixture (1 μL) was spotted onto a polished stainless plate (Bruker Daltonics). MS spectra were obtained with an Ultraflex mass spectrometer (Bruker Daltonics) in the positive reflector mode. The glycan structure was determined from the expected m/z of each glycan.

Real-Time PCR. Total RNAs were prepared from three hepatoma cell lines using TRIzol reagent (Invitrogen, Carlsbad, CA), according to the manufacturer's protocol. Real-time PCR analyses were performed using a Smart Cycler II System (Cepheid, Sunnyvale, CA). cDNA synthesis was performed using a SYBR Green Real-time PCR Core Kit (Takara Bio, Inc.), according to the manufacturer's instructions. Each reaction was performed in a total volume of 25 μL, with 1× SYBR Premix Ex Taq, 200 nM primers, 2 μL of a 1:10 dilution of the cDNA, and RNase-free water. The thermal cycling conditions for the real-time PCR were 10 s at 95 °C to activate SYBR Ex Taq, followed by 40 cycles of denaturation for 5 s at 95 °C, and annealing/extension for 20 s at 60 °C. The mean number of cycles required to reach the threshold of fluorescence detection was calculated for each sample and glyceraldehyde 3-phosphate dehydrogenase expression was quantified for normalization of the amount of cDNA in each sample. The specificity of the amplified product was monitored using its melting curve. The real-time PCR primers were purchased from Takara Bio, Inc. (Shiga, Japan). All primers used in this study are listed in Supporting Information Table 1.

Determination of the AFP-L1 to L3 Ratios by LCA-Affinity Electrophoresis. The AFP-L1 to L3 ratios were determined by densitometric analysis involving LCA-affinity electrophoresis. LCA-affinity electrophoresis images were captured with a ChemiDoc imaging system and analyzed with Quantity One software (Bio-Rad, Hercules CA). LCA-affinity electrophoresis was performed several times and representative results are presented.

Results

Establishment of Huh7-Derived Cell Lines. AFP-L3 is a core-fucosylated AFP and is classified as being LCA-reactive, whereas AFP-L2 is categorized as being weakly LCA-reactive.[29] The LCA reactivity of an AFP is determined by its glycan structure, which in turn is controlled by the activities of various glycosyltransferases. FUT8 catalyzes the transfer of core-fucose to the innermost GlcNAc. FUT8 and core-fucosylated proteins reportedly are increased in patients with HCC.[30,31] In addition, other glycosyltransferases, that is, GnT-III and GnT-V, are elevated in various cancers, including HCC.[32,33] To understand the relationship between glycosyltransferase activities and the glycan structure of an AFP, especially of AFP-L2 and -L3, the glycan structures of AFPs from several glycosyltransferase-transfected cell lines were determined. The effect of bisecting GlcNAc- and branching-structures on AFPs was the primary focus of this study. Huh7 cells were selected for this study, because this cell line expresses lower levels of GnT-III and GnT-V than the other hepatoma cell lines examined—HepG2 and Huh6 (Supporting Information Figure 2). To modify the AFP glycan structures, glycosyltransferases were transiently or stably expressed in Huh7 cells. GnT-III was introduced retrovirally to allow incorporation of the bisecting GlcNAc structure. Huh7 cells were infected with an adenovirus harboring the human GnT-V gene to obtain the branching structure. As Huh7 cells endogenously express a high level of *FUT8*, which catalyzes the addition of core-fucose to AFPs, expression of FUT8 was suppressed by introduction of siRNA against the *FUT8* gene. No morphological changes were observed in any of the cell lines (data not shown). As shown in Figure 1, glycosyltransferase expression was confirmed by Western blot analysis with the corresponding antibodies. Huh7*GnTIII* and Huh7*GnTV* cells expressed substantial amounts of the respective proteins (Figure 1B and C). Modifications to glycan structures were verified with lectin and E_4-PHA for GnT-III, L_4-PHA for GnT-V, and AOL[25,26] for FUT8 (Figure 1). As expected, Huh7*GnT-III* and Huh7*GnT-V* cells showed stronger reactivity to E_4-PHA and L_4-PHA, respectively. FUT8 was barely detectable in Huh7*FUT8*KD cells, and AOL lectin blotting clearly showed the reduction of core-fucose in this cell line (Figure 1A).

LCA-Sepharose Chromatography and LCA-Affinity Electrophoresis. An AFP was purified from conditioned medium of each cell line as described under Materials and Methods. As shown in Supporting Information Figure 1, the purities of the AFPs secreted by the various cell lines were comparable. To confirm efficient PNGase digestion, a PNGase-treated AFP (AFP from Huh7*GnT-V* as a representative) was loaded in the last lane (Supporting Information Figure 1). After PNGase treatment, most AFPs migrated faster than non-PNGase-treated AFPs, indicating that PNGase sufficiently released *N*-glycans from AFPs.

AFP-L3 and -L2 were separated as described under Materials and Methods. To confirm the purities of LCA-bound AFP, AFP-L2 and -L3, each sample was subjected to treatment with an AFP Differentiation Kit L (Wako Pure Chemicals) (Figure 2A). The AFPs from parental Huh7 cells gave two bands, that is, mostly AFP-L3 with a small amount of AFP-L1; however, no AFP-L2 was detected. In contrast, the LCA-purified AFPs

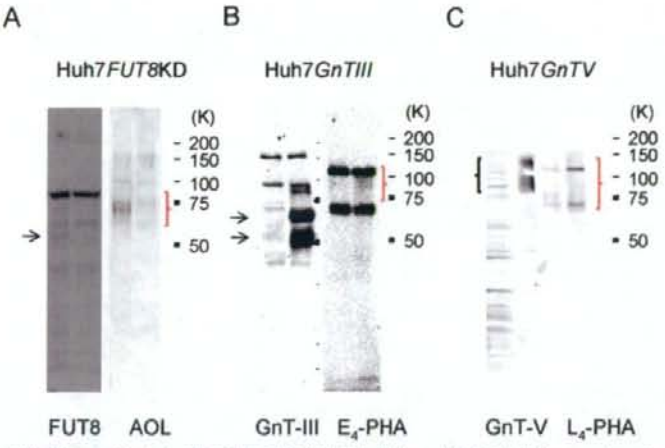

Figure 1. Characterization of Huh7 transfectants. Huh7*FUT8*KD, Huh7*GnT-III*, and Huh7*GnT-V* were characterized by Western blotting with anti-glycosyltransferase antibodies, and with AOL, E_4-PHA, and L_4-PHA, respectively. Parental Huh7 cells were used as a control in each case. (A) Huh7*FUT8*KD cells were probed with anti-FUT8 antibodies and AOL lectin. (B) Huh7*GnT-III* cells were probed with anti-GnT-III antibodies and E_4-PHA. (C) Huh7*GnT-V* cells were probed with anti-GnT-V antibodies and L_4-PHA. Arrows indicate proteins probed with the respective antibodies except for GnT-V. GnT-V and proteins reacting to the respective lectins are also indicated.

comprised only AFP-L3, as expected. AFP-L1 was apparently increased (from 18 to 30% of total AFP) in Huh7*FUT8KD*-derived AFPs. This finding was somewhat surprising, because the suppression of both the Fut8 transcript and protein levels was less than 20%. Apparently, residual FUT8 was sufficient to fucosylate AFPs. The most significant change in the AFP pattern was seen for the AFP purified from Huh7*GnT-III* cells. For this cell line, the mobility of the upper band was apparently faster than that of AFP-L3 from Huh7 cells, but was slower than that of the lower band, AFP-L1. This pattern is characteristic of AFP-L2. Frequently, the AFPs from Huh7*GnT-III* cells showed this distinctive pattern, which is characteristic of AFP-L2 (Figure 2B). Therefore, it was concluded that Huh7*GnT-III* cells produce AFP-L2 rather than AFP-L3. As for AFPs from Huh7*GnT-V* cells, no remarkable change was observed, expect for a slight increase in AFP-L1. The ratio of AFP-L1 to -L3 for each AFP is summarized in Figure 3. All LCA-purified AFPs appeared as one band, corresponding to AFP-L3 or -L2, indicating successful exclusion of AFP-L1 from the total AFPs. Taken together, these results indicate that alteration of glycosyltransferase activities, especially those of FUT8 and GnT-III, strongly affected the pattern on LCA-affinity electrophoresis.

***N*-Glycan Analysis of AFPs from Huh7 Derivatives.** Manipulation of glycosyltransferases in Huh7 cells resulted in changes in the amounts of AFP-L1, L2, and L3, as shown in Figure 3. To elucidate the relationship between AFP-L1 to L3 and glycan structures, the *N*-glycans derived from purified AFPs and from LCA-bound AFPs were determined for each cell type. To focus on the core structure, the terminal sialic acids of PA-glycans were removed by acid treatment. First, the AFPs from parental Huh7 cells were analyzed. A representative chromatogram of the AFPs from Huh7 cells is shown in Figure 4A. Essentially, five types of glycans were detected in Huh7 cells, as shown in Figure 4A and C. Except for a biantennary glycan, G2-bi, all the glycans were core-fucosylated. Although a noncore-fucosylated triantennary (GG2-tri) glycan was also detected on MALDI-TOF analysis, it was not included because it was present in only a very small amount (less than 2%). The biantennary glycans with core-fucose, G2F-bi glycans were the most abundant glycan type, comprising more than 70% of the total glycans (Figures 4 and 6B). The G2-bi glycan comprised less than 10%. The structure of the GnF glycan was deduced from the retention time, the results of digestion with β-galactosidase and exo-β-hexosaminidase, and the intensity in the MS spectrum (Figure 4B and C). The corresponding MALDI-TOF MS spectra are shown in Figure 4B. In addition, bisecting biantennary G2(Gn)F-bi and triantennary glycans with core-fucose GG2F-tri were detected in the amounts of 6 and 9%, respectively (Figure 6B). GG2F-tri reportedly exists in AFPs from both HCC and gallbladder carcinomas.[16] GnF, G2F-, G2(Gn)F-bi and GG2F-tri glycans were core-fucosylated, and comprised 95% of the total glycans. Given that all core-fucosylated glycans are included in AFP-L3, the ratio of core-fucosylated glycans was found to be much greater than that of AFP-L3 (82%) on LCA-affinity electrophoresis (Figure 3). This discrepancy was resolved by analyzing LCA-bound glycans. A chromatograph of LCA-bound glycans from Huh7 cells was superimposed on that of total glycans (Figure 5A). Three of the five types of glycans, GnF, G2F-bi and G2(Gn)F-bi glycans, were recovered from the LCA-bound fraction here. GG2F-tri glycan was not found in LCA-bound glycans, but this finding can be explained by the specificity of LCA for glycans. Kornfeld et al. reported that a β−1,4 branched GlcNAc structure at an α-mannose in the GG2F-tri glycan impairs the binding of core-fucosylated glycans to LCA.[34] Taken together, the results of this study show that the AFP-L3 glycans from Huh7 cells are composed of GnF, G2F-bi and G2(Gn)F-bi glycans. The total amount of these three glycans was 86%, consistent with the 82% obtained for AFP-L3 (Figures 3 and 6B).

Glycans from other cell types were also analyzed. HPLC chromatograms of total and LCA- bound AFPs are shown in Figure 5B−D. The superimposed chromatograph (shown in red) is that for LCA-bound AFPs. The glycan structures in Huh7*FUT8*KD cells were similar to those in Huh7 ones, in both total and LCA-bound glycans, except that the amount of the G2F-bi glycan decreased from 71 to 53% (Figure 6B). Proportionally, the G2-

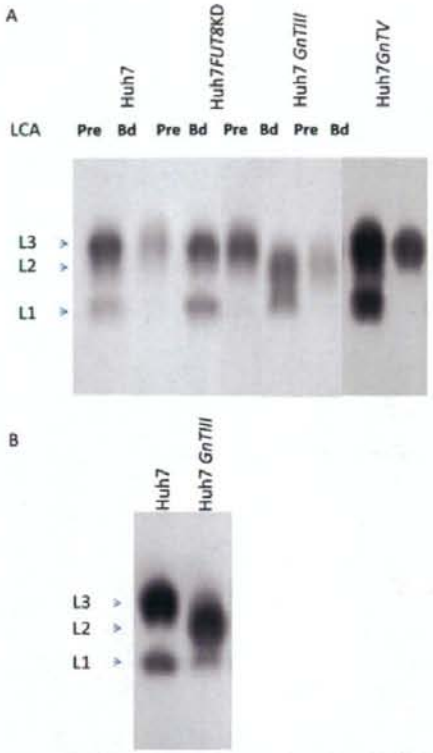

Figure 2. LCA-affinity electrophoresis of total and LCA-bound AFPs. (A) AFPs and LCA-Sepharose bound-AFPs from each cell line were subjected to LCA- affinity electrophoresis using an AFP Differentiation Kit L (Wako Pure Chemicals). Pre and Bd denote total AFPs before LCA-Sepharose chromatography and LCA-Sepharose bound-AFPs, respectively. (B) LCA-affinity electrophoresis of AFPs from Huh7 and Huh7*GnT-III* cells. AFPs from Huh7*GnT-III* cells frequently appeared as "AFP-L2". The bands corresponding to AFP-L1 to L3 are indicated by arrows.

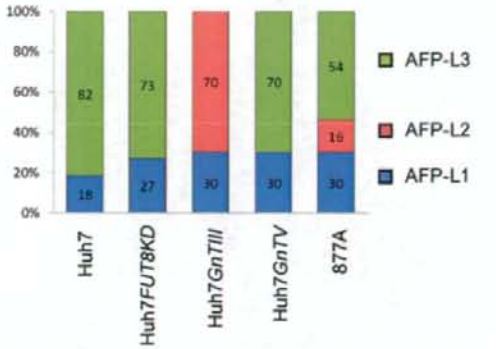

Figure 3. Ratios of AFP-L1 to L3 in each AFP. Ratios were calculated by densitometric analysis of the results of LCA electrophoresis in Figures 2 and 7. The values are expressed as % of total AFPs. The numbers in the columns are % of each AFP fraction (L1 to L3, respectively). In every column, the total of AFP-L1 to -L3 was 100%. Blue bars, AFP-L1; red bars, AFP-L2; green bars, AFP-L3, as indicated in the explanatory notes.

bi glycan increased, from 5 to 14%. Conceivably, the results of the present study show that FUT8 expression regulates, in part, the core-fucosylation of AFPs.

As shown in Figure 5A and C, GnT-III overexpression affected the composition of AFP glycans, as well as the results of LCA-affinity electrophoresis. The G2(Gn)F-bi glycan comprised more than 70 and 90% of the total and LCA-bound AFPs, respectively (Figure 6B). The amount of G2(Gn)F-bi glycan corresponded closely with that of AFP-L2, as shown in Figures 3 and 6B, strongly suggesting that the amount of AFP-L2 is closely associated with GnT-III expression. The bisecting GlcNAc structures in core-fucosylated glycans lower the affinity of the glycans for LCA, but they do not completely abrogate it. Surprisingly, the amount of the bisecting biantennary glycan without core-fucose, the G2(Gn)-bi glycan, did not increase as much as that of the G2(Gn)F-bi glycan did.

As expected, GnT-V expression resulted in an increase in the β-1,6-linked GlcNAc residues on the Man α1,6-arm branched triantennary glycans with core-fucose (G2GF-tri), comprising 43% of the total glycans (Figures 5D and E, and 6B). Introduction of GnT-V converted the G2F-bi glycan in the G2GF-tri glycan. The nonfucosylated one, the G2G-tri glycan, was observed slightly, comprising 8% (Figures 5D and 6B). No other changes were observed for this cell line. It is noteworthy that the "G2GF-tri" glycan was efficiently recovered in the glycans derived from LCA-bound AFPs in contrast to the "GG2F-tri" glycan that was not recovered (Figures 5A,B and 6B). Again, this finding was also consistent with the LCA-binding specificity for triantennary glycans with core-fucose.[34] It is not known why the AFP-L3 amount in this cell line, 70%, was much lower than the total amount of core-fucosylated glycans, 88%; G2F-bi, 38% G2(Gn)F-bi, 7%, and G2GF-tri, 43% (Figures 3 and 6B).

The yield of G2GF-tri glycans was higher than that of G2F-bi glycans. However, it is not clear whether the affinity of LCA for G2GF-tri glycans is higher than that for G2F-bi glycans. Direct measurement of the affinities of G2F-bi and G2GF-tri glycans for LCA is required.

In contrast to the cases of GnT-III overexpression and FUT8 knock down, the G2(Gn)F-bi glycan on GnT-V overexpression was not efficiently recovered in the LCA-bound AFPs, as shown in Figures 5D and 6B, comprising 7% and 0% of the total and the LCA-bound glycans, respectively. At present, we cannot explain this.

Taken together, the results for Huh7 transfectants can be summarized as follows: (1) suppression of *FUT8* expression is directly associated with that of AFP-L3 and core-fucosylated glycans; (2) introduction of a bisecting GlcNAc structure transforms the G2F-bi glycan into a G2(Gn)F-bi glycan with a concurrent increase in the amount of AFP-L2; (3) AFPs with the "G2GF-tri" glycan efficiently bind to LCA and are included in AFP-L3 as well as AFPs with the G2F-bi glycan, but AFPs with the "GG2F-tri" glycan cannot bind to LCA although they are core-fucosylated and are components of AFP-L1. All the symbols used to express the *N*-glycan structures used in this study are summarized in Figure 6A.

Analysis of AFPs from HCC Patients. Finally, AFPs from HCC patients, called 877A, were analyzed, and the correlation between LCA-affinity electrophoresis and glycan structures was examined. All three forms of AFP were evident on LCA-affinity electrophoresis (Figure 7A); it was, however, difficult to clearly differentiate AFP-L3 and -L2. As references, AFPs from patients

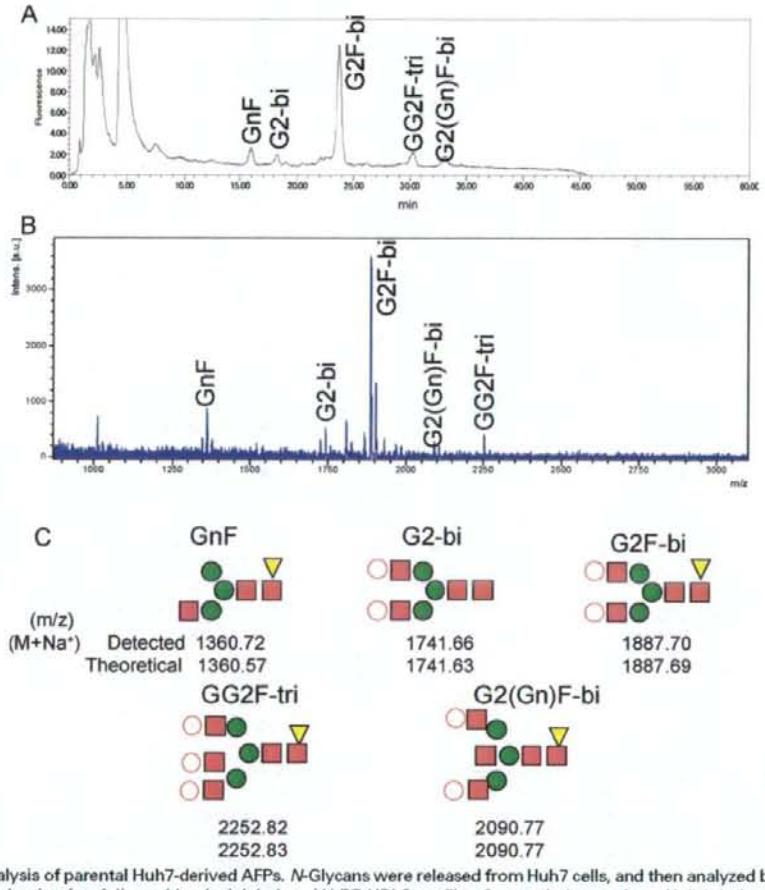

Figure 4. Glycan analysis of parental Huh7-derived AFPs. *N*-Glycans were released from Huh7 cells, and then analyzed by HPLC and MALDI-TOF MS after pyridylamination followed by desialylation. (A) RP-HPLC profile of neutral glycans from Huh7 derived-AFPs. GnF, G2-bi, G2F-bi, GG2F-tri and G2(Gn)F-bi in the chromatogram indicate the peaks for which the structures were determined. Each structure is shown in C. (B) MS spectra of AFPs from Huh7 cells on MALDI-TOF (Ultraflex, Bruker Daltonics). Each peak corresponds to a peak in A. (C) The deduced glycan structures, corresponding to GnF, G2-bi, G2F-bi, GG2F-tri and G2(Gn)F-bi in A and B. Closed triangles, fucose; closed squares, GlcNAc; closed circles, mannose; open circles, galactose. Theoretical and detected *m/z* values of PA-glycans as sodium adducts are given with the structures.

with typical cholangiocarcinomas or HCC were run on the same gels (Figure 7A, lanes 1 and 2). As expected, AFP-L3 and AFP-L1 were the dominant types of AFPs in both the typical HCC patients, and AFP-L3 and AFP-L2 were barely discernible in 877A (Figure 7A). In contrast, AFP-L2 was clearly detected in the AFPs from the cholangiocarcinoma patient, consistent with a previous report (Figure 7A).[3]

Glycans from AFPs and LCA-bound AFPs were analyzed by HPLC and MALDI-TOF. AFP-L2 and -L3 were successfully recovered from the LCA-bound AFPs of 877A (Figure 7A). As shown in Figures 6B, and 7B and C, four types of glycan were detected in the AFPs of 877A, that is, GnF, G2-bi, G2F-bi and G2(Gn)F-bi glycans. No triantennary glycan was detected. Among the four types of glycan observed, the GnF, G2F-bi, and G2(Gn)F-bi glycans were found in the LCA-bound AFPs. In particular, GnF and G2F-bi glycans were efficiently recovered. The amounts on LCA-affinity electrophoresis and the glycan structure analysis results were as follows: AFP-L3, 54%; AFP-L2, 16%; AFP-L1, 30%; fucosylated glycans, GnF and G2F-bi, 70%; bisecting and core-fucosylated glycan, G2(Gn)F-bi, 14%; and, nonfucosylated glycan, G2-bi, 16% (Figures 3 and 6B). As seen on Huh7 analyses, the amount for AFP-L1 was frequently greater than those for the nonfucosylated glycans. Nonetheless, LCA-affinity electrophoresis and glycan structures were strongly correlated for the AFPs from HCC patients, 877A. The glycan structures and amounts of AFP-L1 to L3 were also compared for two other cases, a nice correlation being shown (data not shown).

Conclusions

Five types of AFP from Huh7 transfectants and HCC patients (877A) were analyzed. There were strong correlations between glycan structures and affinity for LCA, and the AFP-L1 to -L3 ratios on LCA-affinity electrophoresis.

The affinity of AFPs for LCA is strongly dependent on the structural modifications of the glycans on the AFPs. In other

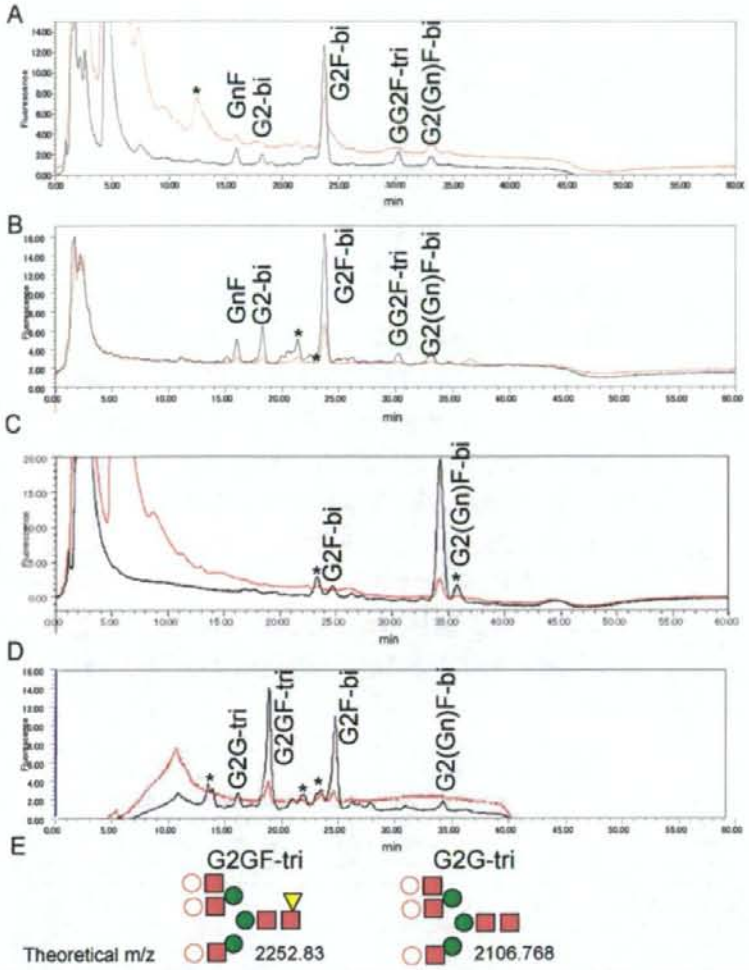

Figure 5. Glycan analysis of AFPs and LCA-Sepharose bound-AFPs from Huh7 transfectants. *N*-Glycans derived from AFPs and LCA-Sepharose bound-AFPs from Huh7 tranfectants were analyzed as in Figure 4. Chromatograms of LCA-bound AFPs are superimposed on those of total AFPs. Black lines, total AFPs; red lines, LCA-bound AFPs. GnF, G2-bi, G2F-bi, GG2F-tri and G2(Gn)F-bi on the peaks represent the glycan structures, as described in Figure 4C. Asterisks indicate false peaks, which are neither reproducible nor overlapped with any known standard *N*-glycans. (A) Huh7; (B) Huh7*FUT8*KD; (C) Huh7*GnT-III*; (D) Huh7*GnT-V*. The structures of the glycans denoted as G2GF-tri and G2G-tri are shown in E. Theoretical *m/z* values of PA-glycans as sodium adducts are given under the structures.

words, *N*-glycan moieties determine the affinity of AFPs for LCA and the LCA-affinity electrophoresis pattern. LCA specifically binds to biantennary glycans with either a fucose at the proximal GlcNAc of the trimannosyl core and/or to ones with both a fucose and a bisecting GlcNAc[34,35] (G2F-bi and G2(Gn)F-bi glycans in this study). In addition, AFPs with a G2F-bi glycan bound to LCA with the same efficiency as ones with a GnF glycan. In contrast, AFPs from Huh7*GnT-III* cells, the majority of which comprised G2(Gn)F-bi glycans, showed faster mobility on LCA-affinity electrophoresis, indicating a weaker interaction with LCA. AFP-L2 was correlated strongly with GnT-III expression and its product—a G2(Gn)F-glycan. As a GnT-III-transferred-GlcNAc is located within the trimannose core to form a bisecting GlcNAc, the resulting structural conformation change may lower the affinity of LCA for *N*-glycans, leading to a conversion of AFP-L3 into AFP-L2. Because the introduction of a bisecting GlcNAc into *N*-glycans inhibits the FUT8 action,[36] core-fucosylation may precede the transfer of the bisecting GlcNAc. The location of each glycosyltransferase in the Golgi apparatus must be elucidated to answer this question. Nonetheless, this study clearly showed that the AFP with a G2(Gn)F-bi glycan is, in fact, AFP-L2, which reacts weakly with LCA.

The glycan structures of human AFPs have been reported by several groups, including Yoshima et al.,[10] Yamashita et al.,[12] and Aoyagi et al.[16] The former two groups analyzed total *N*-glycans, and the latter one analyzed *N*-glycans with

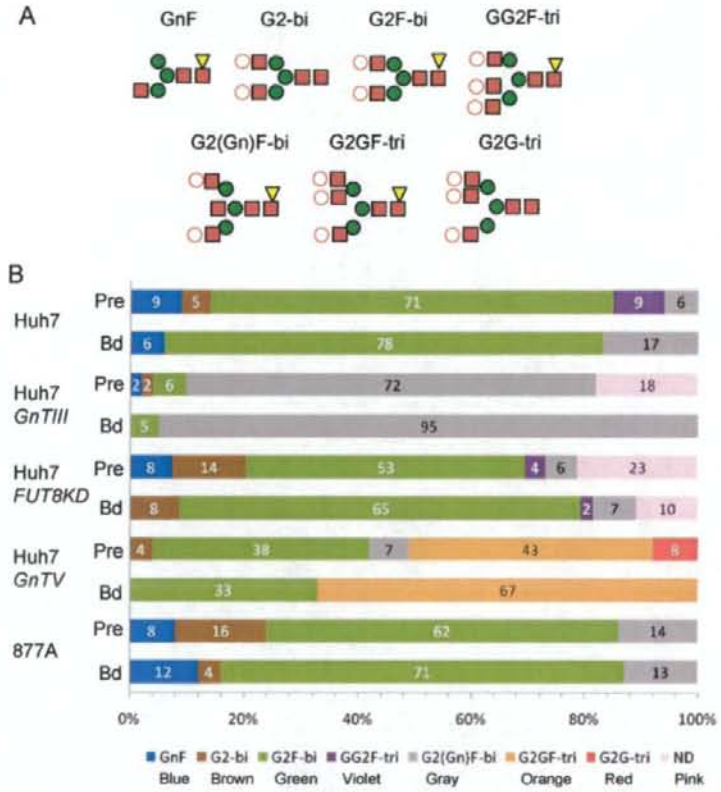

Figure 6. Ratios of major *N*-glycans of AFPs in Huh7 transfectants and HCC patients (877A). (A) Schematic structures of *N*-glycans expressed by symbols, GnF, G2F-bi, G2-bi, GG2F-tri, and G2(Gn)F-bi. This is a summary of Figures 4C and 5E, and theoretical *m/z* values are referred in these Figures. The symbols are explained in Figure 4. (B) Percentages of seven major *N*-glycans in AFPs from Huh7 cells and 877A. "Pre" and "Bd" indicate percentage (%) of *N*-glycans found in total AFPs and LCA bound AFPs, respectively. The percentage of each glycan is indicated in the respective column. An explanatory note is given below the columns. As given, blue, GnF; brown, G2-bi; green, G2F-bi; violet, GG2F-tri; gray, G2(Gn)F-bi; orange, G2GF-tri; red, G2G-tri; pink, ND, not determined. The total of *N*-glycans was 100% in each sample. Pre and Bd were explained in Figure 2.

the combination of LCA and ConA. Yoshima et al. and Yamashita et al. detected two primary types of glycans, biantennary and core-fucosylated biantennary ones, that is, G2-bi and G2F-bi glycans, although they reported that each type was composed of differently sialylated species. In contrast, Aoyagi et al. detected tri- glycans with and without a fucose at the innermost GlcNAc, i.e. GG2- and GG2F-tri glycans. They detected AFPs with a GG2F-tri glycan in the ConA lectin-nonreactive/LCA-nonreactive fraction, which might correspond to the AFP-L1 in the present study. In the present study, no triantennary glycans, with or without core-fucose, were detected in the AFPs from HCC patients. In contrast, the AFPs from parental Huh7 cells contained a GG2F-tri glycan, as seen in the study of Aoyagi et al. Huh7*GnT-V* cells produced AFPs with a core-fucosylated -tri glycan, G2GF-tri glycan. The present study clearly indicated that an AFP with a GG2F-tri glycan hardly binds to LCA and is probably best classified as AFP-L1, which is again compatible with Aoyagi et al.'s study. On the contrary, we clearly showed for the first time that an AFP with a G2GF-tri glycan binds to LCA and is AFP-L3; although, it sometimes is difficult to clearly differentiate AFP-L2 and -L3.

The glycan structures of AFPs were highly correlated with glycosyltransferase activities,[18] FUT8 catalyzes the transfer of L-fucose to the innermost GlcNAc of an *N*-glycan.[9,36] Increased fucosyltransferase activity of either FUT8 or FX, GDP-4-keto-6-deoxy-D-mannose-3,5-epimerase-4-reductase, led to an increase in AFP-L3.[37,38] In the present study, the Huh7*FUT8*KD transfectants also showed that a reduction of *FUT8* leads directly to a decreased amount of AFP-L3. In addition, the concomitant reduction in G2F-bi glycans of AFPs was proportional to the increase in G2-bi glycans. Surprisingly, the reduction in core-fucose of AFPs was not as much as that of AOL staining for the total cell lysates (Figure 1A). This discrepancy between core-fucosylation of AFPs, secreted proteins, and cell lysates might be explained by the role of core-fucose in exocytosis.[12] Core-fucosylated proteins are exclusively secreted from the apical surface of polarized hepatocytes. Nonetheless, this is the first study to establish directly the relationship between glycosyltrans-

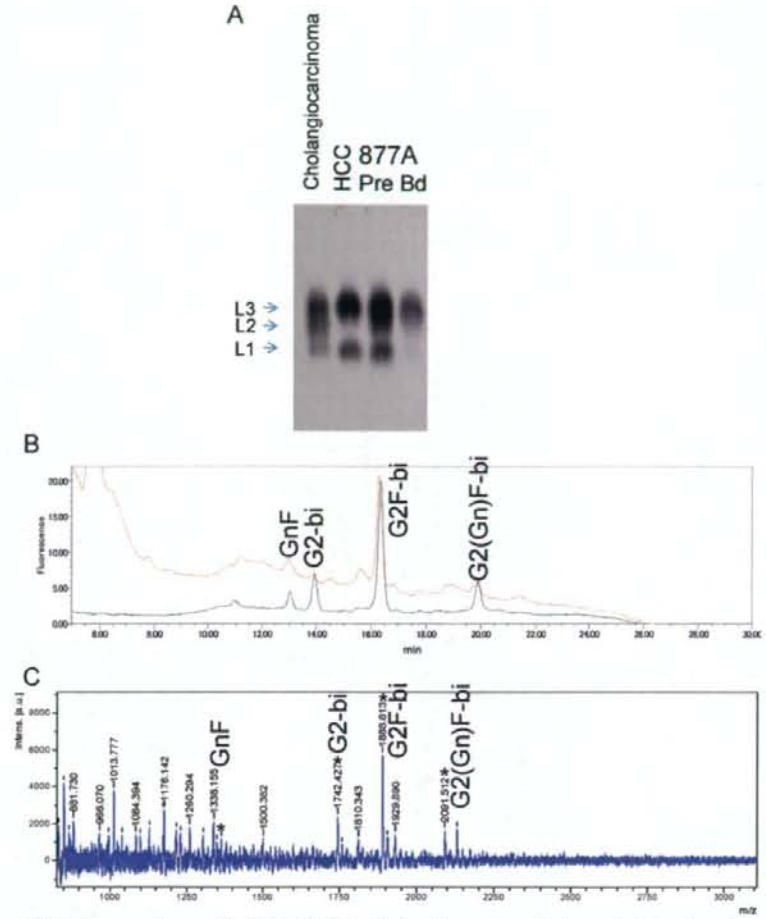

Figure 7. Analysis of AFPs from patients with HCC. (A) LCA-affinity electrophoresis. Lane 1, AFPs from a patient with a typical cholangiocarcinoma; lane 2, AFPs from a patient with HCC; lanes 3 and 4, total and LCA-Sepharose bound-AFPs from the HCC patients (877A) analyzed in this study, respectively. Pre and Bd were explained in Figure 2. (B) HPLC chromatograms of neutral glycans derived from total and LCA-bound AFPs of 877A. Chromatograms of PA-glycans derived from total and LCA-bound AFPs are shown in black and red, respectively. (C) MALDI-TOF MS analysis of *N*-glycans of AFPs from 877A. The structure of each glycan is given in Figures 4C, 5E and 6A. The spectra being focused on is indicated by asterisks.

Table 2. *N*-Glycans of AFPs Found in AFP-L1 to -L3 in This Study

	AFP-L1	AFP-L2	AFP-L3
Associated enzymes[a]	GnT-IV, V FUT8	GnT-III FUT8	GnT-V FUT8
N-Glycans	G2-bi, G2G-tri, GG2F-tri	G2(Gn)F-bi	GnF-bi, G2F-bi, G2GF-tri

[a] The enzymes studied here and involved in the formation of the *N*-glycans indicated. AFP-L1 to -L3 correspond to those in Figures 2 and 3. It is intriguing that GG2F-tri is present in AFP-L1 but not in AFP-L3, despite core-fucosylation.

ferase expression and AFP-L1 to L3 at the structural level (see Table 2 for a summary of the results). Because many tumor markers are carbohydrate antigens, such as CA19-9, CA15-3, and SSEA-1,[39] systematic glycoproteomic analysis of these bio markers, as we showed in this study, will facilitate understanding of the etiologies of various diseases.

Acknowledgment. We thank Eriko Sasabe, Mami Nishikawa and Kay Mikami for their excellent assistance. A part of this work was supported by the 21st Century Center of Excellence (COE) Program of the Ministry of Education, Culture, Sports, Science, and Technology of Japan, the Core Research for Evolutional Science and Technology (CREST), and the Core to Core Program (JSPS).

Supporting Information Available: Figures of the purities of AFPs purified from Huh7 transfectants AFP from each transfectant was subjected to SDS-PAGE followed by CBB staining and real-time PCR analysis of glycosyltransferase expression in Huh7 cells; table of primer sequences used for

real-time PCR. This material is available free of charge via the Internet at http://pubs.acs.org.

References

(1) Morinaga, T.; Sakai, M.; Wegmann, T. G.; Tamaoki, T. Primary structures of human alpha-fetoprotein and its mRNA. *Proc. Natl. Acad. Sci. U.S.A.* **1983**, *80* (15), 4604–8.

(2) Taketa, K. Alpha-fetoprotein: reevaluation in hepatology. *Hepatology* **1990**, *12* (6), 1420–32.

(3) Taketa, K.; Sekiya, C.; Namiki, M.; Akamatsu, K.; Ohta, Y.; Endo, Y.; Kosaka, K. Lectin-reactive profiles of alpha-fetoprotein characterizing hepatocellular carcinoma and related conditions. *Gastroenterology* **1990**, *99* (2), 508–18.

(4) Taketa, K.; Endo, Y.; Sekiya, C.; Tanikawa, K.; Koji, T.; Taga, H.; Satomura, S.; Matsuura, S.; Kawai, T.; Hirai, H. A collaborative study for the evaluation of lectin-reactive alpha-fetoproteins in early detection of hepatocellular carcinoma. *Cancer Res.* **1993**, *53* (22), 5419–23.

(5) Kuromatsu, R.; Tanaka, M.; Tanikawa, K. Serum alpha-fetoprotein and lens culinaris agglutinin-reactive fraction of alpha-fetoprotein in patients with hepatocellular carcinoma. *Liver* **1993**, *13* (4), 177–82.

(6) Khien, V. V.; Mao, H. V.; Chinh, T. T.; Ha, P. T.; Bang, M. H.; Lac, B. V.; Hop, T. V.; Tuan, N. A.; Don, L. V.; Taketa, K.; Satomura, S. Clinical evaluation of lentil lectin-reactive alpha-fetoprotein-L3 in histology-proven hepatocellular carcinoma. *Int. J. Biol. Markers* **2001**, *16* (2), 105–11.

(7) Oka, H.; Saito, A.; Ito, K.; Kumada, T.; Satomura, S.; Kasugai, H.; Osaki, Y.; Seki, T.; Kudo, M.; Tanaka, M. Multicenter prospective analysis of newly diagnosed hepatocellular carcinoma with respect to the percentage of Lens culinaris agglutinin-reactive alpha-fetoprotein. *J. Gastroenterol. Hepatol.* **2001**, *16* (12), 1378–83.

(8) Tada, T.; Kumada, T.; Toyoda, H.; Kiriyama, S.; Sone, Y.; Tanikawa, M.; Hisanaga, Y.; Kitabatake, S.; Kuzuya, T.; Nonogaki, K.; Shimizu, J.; Yamaguchi, A.; Isogai, M.; Kaneoka, Y.; Washizu, J.; Satomura, S. Relationship between Lens culinaris agglutinin-reactive alpha-fetoprotein and pathologic features of hepatocellular carcinoma. *Liver Int.* **2005**, *25* (4), 848–53.

(9) Uozumi, N.; Yanagidani, S.; Miyoshi, E.; Ihara, Y.; Sakuma, T.; Gao, C. X.; Teshima, T.; Fujii, S.; Shiba, T.; Taniguchi, N. Purification and cDNA cloning of porcine brain GDP-L-Fuc:N-acetyl-beta-D-glucosaminide alpha1-->6fucosyltransferase. *J. Biol. Chem.* **1996**, *271* (44), 27810–7.

(10) Yoshima, H.; Mizuochi, T.; Ishii, M.; Kobata, A. Structure of the asparagine-linked sugar chains of alpha-fetoprotein purified from human ascites fluid. *Cancer Res.* **1980**, *40* (11), 4276–81.

(11) Yamashita, K.; Hitoi, A.; Tsuchida, Y.; Nishi, S.; Kobata, A. Sugar chain of {alpha}-fetoprotein produced in human yolk sac tumor. *Cancer Res.* **1983**, *43* (10), 4691–4695.

(12) Yamashita, K.; Taketa, K.; Nishi, S.; Fukushima, K.; Ohkura, T. Sugar chains of human cord serum {alpha}-fetoprotein: characteristics of N-linked sugar chains of glycoproteins produced in human liver and hepatocellular carcinomas. *Cancer Res.* **1993**, *53* (13), 2970–2975.

(13) Taketa, K.; Ichikawa, E.; Sato, J.; Taga, H.; Hirai, H. Two-dimensional lectin affinity electrophoresis of alpha-fetoprotein: characterization of erythroagglutinating phytohemagglutinin-dependent microheterogeneity forms. *Electrophoresis* **1989**, *10* (12), 825–9.

(14) Kinoshita, N.; Suzuki, S.; Matsuda, Y.; Taniguchi, N. Alpha-fetoprotein antibody-lectin enzyme immunoassay to characterize sugar chains for the study of liver diseases. *Clin. Chim. Acta* **1989**, *179* (2), 143–51.

(15) Taketa, K.; Ichikawa, E.; Akamatsu, K.; Ohta, Y.; Sekiya, C.; Namiki, M.; Takami, H.; Kaneda, H.; Higashino, K.; Taga, H.; et al. Increased asialo-alpha-fetoprotein in patients with alpha-fetoprotein-producing tumors: demonstration by affinity electrophoresis with erythroagglutinating phytohemagglutinin of Phaseolus vulgaris lectin. *Tumour Biol.* **1985**, *6* (6), 533–44.

(16) Aoyagi, Y.; Suzuki, Y.; Igarashi, K.; Saitoh, A.; Oguro, M.; Yokota, T.; Mori, S.; Suda, T.; Isemura, M.; Asakura, H. Carbohydrate structures of human alpha-fetoprotein of patients with hepatocellular carcinoma: presence of fucosylated and non-fucosylated triantennary glycans. *Br. J. Cancer* **1993**, *67* (3), 486–92.

(17) Mita, Y.; Aoyagi, Y.; Suda, T.; Asakura, H. Plasma fucosyltransferase activity in patients with hepatocellular carcinoma, with special reference to correlation with fucosylated species of alpha-fetoprotein. *J. Hepatol.* **2000**, *32* (6), 946–54.

(18) Ohno, M.; Nishikawa, A.; Koketsu, M.; Taga, H.; Endo, Y.; Hada, T.; Higashino, K.; Taniguchi, N. Enzymatic basis of sugar structures of alpha-fetoprotein in hepatoma and hepatoblastoma cell lines: correlation with activities of alpha 1−6 fucosyltransferase and N-acetylglucosaminyltransferases III and V. *Int. J. Cancer* **1992**, *51* (2), 315–7.

(19) Taketa, K.; Liu, M.; Taga, H. Interaction of lectins with their ligand carbohydrate of alpha-fetoprotein: Analysis by mixed-lectin affinity electrophoresis. *Electrophoresis* **1996**, *17* (3), 483–8.

(20) Li, W.; Nakagawa, T.; Koyama, N.; Wang, X.; Jin, J.; Mizuno-Horikawa, Y.; Gu, J.; Miyoshi, E.; Kato, I.; Honke, K.; Taniguchi, N.; Kondo, A. Down-regulation of trypsinogen expression is associated with growth retardation in alpha1,6-fucosyltransferase-deficient mice: attenuation of proteinase-activated receptor 2 activity. *Glycobiology* **2006**, *16* (10), 1007–19.

(21) Takahashi, T.; Ikeda, Y.; Miyoshi, E.; Yaginuma, Y.; Ishikawa, M.; Taniguchi, N. alpha1,6fucosyltransferase is highly and specifically expressed in human ovarian serous adenocarcinomas. *Int. J. Cancer* **2000**, *88* (6), 914–9.

(22) Kitada, T.; Miyoshi, E.; Noda, K.; Higashiyama, S.; Ihara, H.; Matsuura, N.; Hayashi, N.; Kawata, S.; Matsuzawa, Y.; Taniguchi, N. The addition of bisecting N-acetylglucosamine residues to E-cadherin down-regulates the tyrosine phosphorylation of beta-catenin. *J. Biol. Chem.* **2001**, *276* (1), 475–80.

(23) Sasai, K.; Ikeda, Y.; Tsuda, T.; Ihara, H.; Korekane, H.; Shiota, K.; Taniguchi, N. The critical role of the stem region as a functional domain responsible for the oligomerization and Golgi localization of N-acetylglucosaminyltransferase V. The involvement of a domain homophilic interaction. *J. Biol. Chem.* **2001**, *276* (1), 759–65.

(24) Cummings, R. D.; Kornfeld, S. Characterization of the structural determinants required for the high affinity interaction of asparagine-linked oligosaccharides with immobilized Phaseolus vulgaris leukoagglutinating and erythroagglutinating lectins. *J. Biol. Chem.* **1982**, *257* (19), 11230–11234.

(25) Matsumura, K.; Higashida, K.; Ishida, H.; Hata, Y.; Yamamoto, K.; Shigeta, M.; Mizuno-Horikawa, Y.; Wang, X.; Miyoshi, E.; Gu, J.; Taniguchi, N. Carbohydrate binding specificity of a fucose-specific lectin from Aspergillus oryzae: a novel probe for core fucose. *J. Biol. Chem.* **2007**, *282* (21), 15700–15708.

(26) Ishida, H.; Moritani, T.; Hata, Y.; Kawato, A.; Suginami, K.; Abe, Y.; Imayasu, S. Molecular cloning and overexpression of fleA gene encoding a fucose-specific lectin of Aspergillus oryzae. *Biosci. Biotechnol. Biochem.* **2002**, *66* (5), 1002–8.

(27) Kondo, A.; Hosokawa, Y.; Kiso, M.; Hasegawa, A.; Kato, I. Analysis of oligosaccharides of human IgG from serum of leukemia patients. *Biochem. Mol. Biol. Int.* **1994**, *32* (5), 897–902.

(28) Kondo, A.; Kiso, M.; Hasegawa, A.; Kato, I. Separation of pyridylamino oligosaccharides by high-performance liquid chromatography on an amine-bearing silica column. *Anal. Biochem.* **1994**, *219* (1), 21–5.

(29) Taketa, K.; Hirai, H. Lectin affinity electrophoresis of alpha-fetoprotein in cancer diagnosis. *Electrophoresis* **1989**, *10* (8−9), 562–7.

(30) Hutchinson, W. L.; Du, M. Q.; Johnson, P. J.; Williams, R. Fucosyltransferases: differential plasma and tissue alterations in hepatocellular carcinoma and cirrhosis. *Hepatology* **1991**, *13* (4), 683–8.

(31) Du, M. Q.; Hutchinson, W. L.; Johnson, P. J.; Williams, R. Differential alpha-fetoprotein lectin binding in hepatocellular carcinoma. Diagnostic utility at low serum levels. *Cancer* **1991**, *67* (2), 476–80.

(32) Yao, M.; Zhou, D. P.; Jiang, S. M.; Wang, Q. H.; Zhou, X. D.; Tang, Z. Y.; Gu, J. X. Elevated activity of N-acetylglucosaminyltransferase V in human hepatocellular carcinoma. *J. Cancer Res. Clin. Oncol.* **1998**, *124* (1), 27–30.

(33) Miyoshi, E.; Nishikawa, A.; Ihara, Y.; Gu, J.; Sugiyama, T.; Hayashi, N.; Fusamoto, H.; Kamada, T.; Taniguchi, N. N-acetylglucosaminyltransferase III and V messenger RNA levels in LEC rats during hepatocarcinogenesis. *Cancer Res.* **1993**, *53* (17), 3899–902.

(34) Kornfeld, K.; Reitman, M. L.; Kornfeld, R. The carbohydrate-binding specificity of pea and lentil lectins. Fucose is an important determinant. *J. Biol. Chem.* **1981**, *256* (13), 6633–6640.

(35) Yamamoto, K.; Tsuji, T.; Osawa, T. Requirement of the core structure of a complex-type glycopeptide for the binding to immobilized lentil- and pea-lectins. *Carbohydr. Res.* **1982**, *110* (2), 283–9.

(36) Longmore, G. D.; Schachter, H. Product-identification and substrate-specificity studies of the GDP-L-fucose:2-acetamido-2-deoxy-beta-D-glucoside (FUC goes to Asn-linked GlcNAc) 6-alpha-L-fucosyltransferase in a Golgi-rich fraction from porcine liver. *Carbohydr. Res.* **1982**, *100*, 365–92.

(37) Noda, K.; Miyoshi, E.; Kitada, T.; Nakahara, S.; Gao, C. X.; Honke, K.; Shiratori, Y.; Moriwaki, H.; Sasaki, Y.; Kasahara, A.; Hori, M.; Hayashi, N.; Taniguchi, N. The enzymatic basis for the conversion of nonfucosylated to fucosylated alpha-fetoprotein by acyclic retinoid treatment in human hepatoma cells: activation of alpha1–6 fucosyltransferase. *Tumour Biol.* **2002**, *23* (4), 202–11.

(38) Noda, K.; Miyoshi, E.; Gu, J.; Gao, C. X.; Nakahara, S.; Kitada, T.; Honke, K.; Suzuki, K.; Yoshihara, H.; Yoshikawa, K.; Kawano, K.; Tonetti, M.; Kasahara, A.; Hori, M.; Hayashi, N.; Taniguchi, N. Relationship between elevated FX expression and increased production of GDP-L-fucose, a common donor substrate for fucosylation in human hepatocellular carcinoma and hepatoma cell lines. *Cancer Res.* **2003**, *63* (19), 6282–9.

(39) Freire, T.; Bay, S.; Vichier-Guerre, S.; Lo-Man, R.; Leclerc, C. Carbohydrate Antigens: Synthesis Aspects and Immunological Applications in Cancer. *Mini Rev. Med. Chem.* **2006**, *6*, 1357.

PR700841Q

Functional Proteomics Study Reveals That *N*-Acetylglucosaminyltransferase V Reinforces the Invasive/Metastatic Potential of Colon Cancer through Aberrant Glycosylation on Tissue Inhibitor of Metalloproteinase-1*

Yong-Sam Kim‡, Soo Young Hwang‡, Hye-Yeon Kang‡, Hosung Sohn‡, Sejeong Oh§, Jin-Young Kim¶, Jong Shin Yoo¶, Young Hwan Kim¶, Cheorl-Ho Kim‖, Jae-Heung Jeon, Jung Mi Lee‡‡, Hyun Ah Kang‡‡, Eiji Miyoshi§§, Naoyuki Taniguchi§§, Hyang-Sook Yoo‡, and Jeong-Heon Ko‡¶¶**

N*-Acetylglucosaminyltransferase-V (GnT-V) has been reported to be up-regulated in invasive/metastatic cancer cells, but a comprehensive understanding of how the transferase correlates with the invasive/metastatic potential is not currently available. Through a glycomics approach, we identified 30 proteins, including tissue inhibitor of metalloproteinase-1 (TIMP-1), as a target protein for GnT-V in human colon cancer cell WiDr. TIMP-1 was aberrantly glycosylated as characterized by the addition of β1,6-*N*-acetylglucosamine, polylactosaminylation, and sialylation in GnT-V-overexpressing WiDr cells. Compared with normal TIMP-1, the aberrantly glycosylated TIMP-1 showed the weaker inhibition on both matrix metalloproteinase (MMP)-2 and MMP-9, and this aberrancy was closely associated with cancer cell invasion and metastasis *in vivo* as well as *in vitro*. Integrated data, both of TIMP-1 expression level and aberrant glycosylation, could provide important information to aid to improve the clinical outcome of colon cancer patients. *Molecular & Cellular Proteomics 7:1–14, 2008.

Cancer is a very complicated process, characterized by the uncontrolled, unbalanced overgrowth of malignant cells. The complexity of oncogenic processes and cancer progressions has demanded the discovery of biomarkers with a high sensitivity and specificity for diagnosis, prognosis, diseases monitoring, and therapeutic response prediction. Unfortunately, a discrete biomarker for colon cancer has yet to be discovered, although nearly 800,000 new colorectal cancer cases are thought to globally occur each year, which account for ~10% of all incident cancers, and the mortality from colorectal cancer is estimated at nearly 450,000 per year (1). *MLI1* and *MSH* genes are associated with hereditary non-polyposis colon cancer (2), and the *APC* gene is associated with familial adenomatous polyposis (3), but those factors fail to account for an occurrence of wide range of colon cancer. Moreover, colon cancer is one of the epithelium-derived cancers in which the circumstantial factors govern over hereditary genetic factors. These require a clear marker that serves as tracer molecule for the efficacious treatment of colon cancer.

Recent proteomics have focused on a dynamic alteration of post-translational modification of proteins, and many lines of evidence indicate that changes in post-translational modification of proteins are closely associated with the pathogenic processes of cells. An aberrant glycosylation induced by *N*-acetylglucosaminyltransferase V (GnT-V),[1] is a representative example of such protein modification as is implicated in tumor progression. An increase in β1,6-branching on *N*-linked glycans is associated with metastatic potential of cancer cells (4). Several target molecules for GnT-V were proposed to be involved in cancer progressions, including matriptase (5), β_1 integrin (6), and N-cadherin (7). However, those proteins are membrane-bound proteins and were not demonstrated to be aberrantly glycosylated in sera or tissues of cancer patients. Recent work stresses the discrete roles of the microenviron-

From the ‡Daejeon-KRIBB-Fred Hutchinson Cancer Research Center Research Cooperation Center, **Plant Genome Research Center, ‡‡Protein Therapeutics Research Center, KRIBB, Daejeon 305-806, Korea, §Department of Surgery, College of Medicine, Catholic University of Korea, Inchon 403-720, Korea, ¶Analysis & Measurement Division, Korea Basic Science Institute, P. O. Box 41, Yusong, Daejeon, 305-333, Korea, ‖Department of Biological Sciences, Sungkyunkwan University, Suwon City, Kyunggi-Do 440-746, Korea, and the §§Department of Biochemistry, Osaka University Medical School/Graduate School of Medicine, Suita, Osaka 565-0871, Japan

Received, February 27, 2007, and in revised form, September 12, 2007

¶¶ To whom correspondence should be addressed: Tel.: 82-42-860-4133; Fax: 82-42-879-8119; E-mail: jhko@kribb.re.kr.

[1] The abbreviations used are: GnT-V, *N*-acetylglucosaminyltransferase V; DSA, *Datura stramonium* agglutinin; Gal, galactose; GlcNAc, *N*-acetylglucosamine; L-PHA, phytohemagglutinin-L_4; MMP, metalloproteinase; Neu, *N*-acetylneuraminic acid; TIMP, tissue inhibitor of metalloproteinase; rTIMP-1, TIMP-1 recombinant protein.

ment of tumor cells, referred to as "stroma," and documents its importance in supporting tumor progression (8). Cancer cells modulate their stromal environments by secreting various molecules, including growth factors, proteases, and extracellular matrix molecules (9–11). Many of the secreted proteins are glycoproteins, which prompted us to identify secreted glycoproteins that undergo aberrant glycosylation and are functionally responsible for cancer progression. For this, we adopted proteomics and glycomics techniques in which two-dimensional electrophoresis, lectin blot analysis, and MS-based protein identification were linked. We have previously reported that these approaches allowed us to identify several candidate proteins that are assumed to be involved in progressions of gastric cancer (12) and colon cancer (13) and have validated these approaches for discovery of biomarker by showing the role of aberrant glycosylation of protein tyrosine phosphatase κas an example in cancer cell migration (13). In this article, we report that additional candidate proteins were identified including tissue inhibitor of metalloproteinase-1 (TIMP-1) as the target for GnT-V and, more importantly, that the aberrant glycosylation of TIMP-1 is closely correlated with invasive/metastatic potential of colon cancer cell WiDr.

EXPERIMENTAL PROCEDURES

Establishment of GnT-V and TIMP-1 Transfectants—Recombinant vectors *MGAT5*/pCXN (neo) were transfected into WiDr, a derivative of the human colonic adenocarcinoma cell line HT-29 (14), using Lipofectamine Plus Reagent (Invitrogen) according to the manufacturer's instructions, and the stable transfectants (WiDr:GnT-V) and the control cells (WiDr:mock) were established. TIMP-1 mutant genes were generated using the standard Megaprimer methods, where either or both Asn^{30} and Asn^{78} were changed to Gln. Wild-type *TIMP-1* and the mutant genes were cloned into pcDNA 3.1 hygro(+) plasmid vector (Invitrogen). The cloned vectors were transfected into WiDr: mock or WiDr:GnT-V cells. The stable TIMP-1 transfectants were confirmed by immunoblot analysis. Cells were maintained as monolayer in RPMI 1640 medium containing 10% fetal bovine serum at 37 °C, supplied with 5% CO_2.

Two-dimensional Electrophoresis and Mass Spectrometry—WiDr cells were cultured in a serum-free RPMI 1640 media for 3 days. From the media protein samples were prepared and subjected to two-dimensional electrophoretic analysis as described previously (12). For comparison of the expression level, 50 μg of proteins was minimally labeled with cy3- or cy5-fluorescent dyes following two-dimensional differential in-gel electrophoresis, according to the manufacturer's instructions. Fluorescence was measured with a Typoon 9410 Imager system (GE Healthcare), and an image analysis was performed using a Phoretix software (PerkinElmer Life Sciences). The protein spots of interest were excised, destained, and tryptic-digested using modified porcine trypsin (Promega). If necessary, the recovered peptides were desalted, concentrated using C18 ZipTips (Milliphore), eluted with 50% (v/v) acetonitrile:water, and lyophilized. The lyophilized peptide samples were dissolved in 0.1% formic acid for LC-MS/MS. All MS/MS experiments for peptide identification were performed using a nano-LC/MS system consisting of an ultimate HPLC system and a Q-TOF mass spectrometer (Waters) equipped with a nano-ESI source. Ten microliters of each sample was loaded by an autosampler (Surveyor) onto a C18 trap column (inner diameter, 300 μm; length, 5 mm; particle size, 5 μm; LC Packings) for desalting and concentration at a flow rate of 20 μl/min. Then, the trapped peptides were back flushed and separated on a homemade microcapillary column (length, 150 mm) packed with C18 (particle size, 5 μm) in 75-μm silica tubing (8-μm inner diameter orifice). The mobile phases, A and B, were composed of 0 and 80% acetonitrile, respectively, containing 0.1% formic acid. The gradient began at 5% B for 15 min, ramped to 20% B for 3 min, to 60% for 45 min, to 95% for 2 min, and, finally, to 95% B for 7 min. The column was equilibrated with 5% B for 10 min before the next run. The voltage applied to produce an electrospray was 2.5 kV, and the cone voltage was 30 eV. Argon was introduced as a collision gas at a pressure of 10 pounds per square inch. Data-dependent peak selection of the three most abundant MS ions from MS was used, where the collision energy was increased to 30 eV.

Database Search and Analysis—Peak lists were generated and processed using MassLynx software version 3.5 (Waters). MS spectra were smoothed once using a Savitzky Golary method set as ±3 channels and centered using the top 50% of each peak. The resulting .dta files from each analysis were automatically combined into a single text file. The resulting peak lists were searched against National Center for Biotechnology Information (NCBI) non-redundant database 20051212 (taxonomy, human; entries, 103,913 human sequence entries) using Mascot search engine version 2.0 (Matrix Science). Mascot was used with monoisotopic mass selected, a precursor mass tolerance of ±1.5 Da, and a fragment mass tolerance of ±0.8 Da. Trypsin was selected as the enzyme, with one potential missed cleavage. ESI-QTOF was selected as the instrumental type. Oxidized methionine, pyroglutamate (N-term Q), propioamide cysteine, and carbamidomethylated cystein were chosen as variable modifications. With regards to acceptance criteria for protein identification, those candidates that were identified with 2 or more high scoring peptides from Mascot were selected. High score peptides corresponded to peptides that were above the threshold in Mascot searches ($p < 0.05$, peptide score > 40). Among the candidate proteins, one protein was singled out on the criteria that the theoretical pI and molecular mass closely match the estimated values on a two-dimensional gel and the sequence are more highly covered by the sequenced peptides. All peptide lists were compiled in supplemental Table I. In cases where multispots were identified to be one protein, the peptides of a protein identified with the highest score were listed. All the peptides were checked manually to see if they are found in proteins other than those searched in Mascot engine, and peptides common to different proteins were marked in italic. All identified proteins were checked to contain at least one specific and nonredundant peptide.

Northern Blot Analysis—Total RNA was isolated from the cultured cells using TRIzol (Invitrogen) and quantified spectrophotometrically. RNA samples were fractionated on a 1% formaldehyde agarose gel and transferred to a Hybond-N nylon membrane (Amersham Biosciences). cDNA fragments of the *MGAT5* gene were labeled with [α-^{32}P]dCTP using a Random Primer labeling kit (Stratagene) according to the manufacturer's instructions and hybridized with RNA blots using ULTRAhyb hybridization buffer (Ambion) overnight at 42 °C.

Western and Lectin Blot Analyses—Proteins were resolved on 10–15% SDS-PAGE gels and transferred electrically onto PVDF membranes (Immobilon-P, Millipore). The membranes were blocked in 0.05% Tween 20-TBS containing 5% skim milk (immunoblot) or 3% BSA (lectin blot) and then incubated with primary antibodies or biotin-labeled lectin. After hybridizing with horseradish peroxidase-labeled secondary antibody (Cell Signaling) or horseradish peroxidase-avidin conjugates (Vector Laboratories, Inc.), the membranes were reacted with ECL Western blotting detection reagents (Pharmacia) and exposed to X-ray film for 1–2 min.

Immunoprecipitation—Tissue samples were prepared from resection specimens from colon cancer patients at the Catholic University Hospital (Incheon, Korea) with the patients' agreements. Proteins

extracted in 50 mM Tris-HCl (pH 8.0), 5 mM EDTA, 150 mM NaCl, and 0.1% Nonidet P-40 were immunoprecipitated using monoclonal human TIMP-1 antibody (Santa Cruz Biotechnology). The precipitated complexes were denatured with SDS-PAGE loading buffer.

Protein Purification and Quantification—TIMP-1 was purified on an $IgG_{anti\text{-}TIMP\text{-}1}$-conjugated Sepharose 4B column, prepared by incubating a monoclonal TIMP-1 antibody (Santa Cruz Biotechnology) with CNBr-activated Sepharose 4B at 37 °C for 4 h according to the manufacturer's instructions. The protein concentration of the purified TIMP-1 was determined using a molar extinction coefficient of 26,500 M^{-1} cm^{-1}.

Tumor Cell Migration and Invasion Assay—Cell migration assays were performed using 12-well Transwell chambers (Corning Inc.) with 8 μm-pore size polycarbonate inserts as described previously (6). Cells migrating or invading to the lower surface of the filters were fixed in methanol, stained with Toluidine blue, and counted with a microscope at ×400.

In Vitro Gelatinase Inhibition Assays—The proforms of matrix metalloproteinase (MMP), ProMMP-2 and proMMP-9 (Calbiochem), were activated by incubation with an equal molar ratio of active MMP-3 (Sigma) at 37 °C for 4 h and 1 mM *p*-aminophenylmercuric acetate at 37 °C for 2 h, respectively. The active gelatinases were purified on a gelatin-Sepharose (Sigma) column according to the previous procedures (15). Following the incubation of gelatinases (50 ng) with equal molar ratio of TIMP-1 in 50 mM Tris-HCl buffer (pH 7.5), 150 mM NaCl, 5 mM $CaCl_2$, 0.1 mM $ZnCl_2$, 0.02% Brij-35, and MMP inhibitors at 4 °C for 1 h, fluorogenic substrates DABCYL-GABA-PQGL-E(EDANS)-AK-NH_2 (Calbiochem) was added at 8 μM, and the hydrolysis activity was kinetically measured in an LS 45 Luminescence Spectrometer (PerkinElmer Life Sciences) at an excitation and emission wavelengths of 338 and 495 nm, respectively.

Determination of Kinetic Parameters for TIMP-1-Gelatinase Interaction—Kinetic parameters (k_{on}, k_{off}, K_i) for TIMP-1-gelatinase interaction were determined according to the previous procedure (16) with minor modifications. Briefly, the first-order binding constants (k) were determined under the following conditions. Active gelatinases were added at 1 nM into the reaction mixture containing 8 μM fluorescent substrate and TIMP-1. TIMP-1:mock and TIMP-1:GnT-V were varied from 0 to 6 nM and 0 to 25 nM, respectively. Progress curves were recorded at 37 °C in an LS 45 Spectrometer (PerkinElmer Life Sciences). The curves were fitted to Eq. 1 (12):

$$[P] = v_s t + (v_0 - v_s)(1 - e^{-kt})/k \qquad \text{(Eq. 1)}$$

in which [P] is the product concentration, v_0 and v_s are the initial and steady-state velocities, respectively, and k is pseudo first-order rate constant of inhibition: v_s, and k were calculated with regression method using SigmaPlot (SPSS Science, Inc.). The second-order rate constant (k_{on}) was calculated by the linear regression of k as a function of TIMP-1 concentration.

The k_{off} values were estimated from the time course for the dissociation of the gelatinase-TIMP-1 complex. The complexes were prepared by incubation of equimolar amounts of gelatinases and TIMP-1 (1 μM) at 37 °C for 1 h. Complex dissociation was achieved by diluting the complexes 1,000-fold in a cuvette containing the substrate. After reaching equilibrium, the recorded time-response curves were fitted to Eq. 1. The negative of the obtained values were used as an approximation of k_{off}. The inhibition constants (K_i) were calculated by $K_i = k_{off}/k_{on}$.

Zymography—Latent and active forms of gelatinases were run on 12% SDS-PAGE gel copolymerized with 0.5% (w/v) gelatin and 5 μg/ml of recombinant protein (rTIMP-1) or the mutant proteins. Gelatinases and recombinant proteins in the gel were allowed to bind at 4 °C overnight, and the embedded gelatin was allowed to be hydrolyzed at 37 °C for 12 h in 50 mM Tris-HCl (pH 7.5), 150 mM NaCl, 5 mM $CaCl_2$, 0.1 mM $ZnCl_2$, and 0.02% (w/v) Brij-35 containing, if necessary, gelatinases specific inhibitors or EDTA.

Profiling of N-Glycans of TIMP-1—Profiling of the *N*-glycans of TIMP-1 was performed as described previously (17) with minor modifications. Briefly, about 200 pmol of TIMP-1 purified either from WiDr:mock or WiDr:GnT-V was resolved on a 12% SDS-PAGE gel. The bands corresponding to TIMP-1 were sliced to pieces, washed with 50 mM $NaHCO_3$ buffer (pH 7.0) for 1 h, and dried *in vacuo*. In-gel digestion of *N*-glycans was performed for 18–24 h by treatment with 10 units of PNGase-F in 50 mM $NaHCO_3$ buffer (pH 7.0). The digested *N*-glycans were extracted from the gels on a vortexer twice with 100 μl of water and once with acetonitrile, and, if necessary, the extracted *N*-glycans were further deglycosylated with sialidase and β-galactosidase according to the manufacturer's instructions. Following desalting of the *N*-glycan samples on a graphitized carbon column (Alltech), *N*-acetylneuraminic acids on the glycans were esterified with iodomethane in anhydrous dimethyl sulfoxide at room temperature for 2 h. After unreacted iodomethane was vaporized under nitrogen stream, glycan samples were dried *in vacuo* and reconstituted in 2 μl of 25% acetonitrile. If necessary, glycan samples were desalted with Bio-Rex MSZ 501 (D) ion exchangers (Bio-Rad) prior to reconstitution. The reconstituted samples were mixed with equal volume of matrix consisting of saturated 2,5-dihydroxybenzoic acid and 6-aza-2-thiothymine, and the mixtures were applied on a MALDI MSP 600/96 chip and dried in air. All mass spectra were acquired on a Bruker Daltonics microflex MALDI-TOF mass spectrometer (Bruker Daltonics) using FlexControl software version 2.4 and processed using Flexanalysis software version 2.4 to analyze raw data. Each spectrum was calibrated internally with angiotensin II (average mass of $[M+H]^+$: 1047.20 Da), angiotensin I (1297.51 Da), substance P (1348.66 Da), bombesin (1620.88 Da), ACTH clip 1–17 (2094.46 Da), ACTH clip 18–39 (2466.73 Da), and somatostatin 28 (3149.61 Da) to reach a typical mass measurement accuracy of ±23 parts/million in the 1400–4500 *m/z* range. All samples were irradiated with UV light (337 nm) from an N_2 laser. The neutral and sialylated *N*-glycans after esterification were analyzed at a 20-kV accelerating voltage in the reflectron positive ion mode in which glycans are observed as $[M+Na]^+$ ions. About 200 scans were averaged for each of the spectra. The *N*-glycan structures were deduced from the *m/z* values, which were blasted with a mass tolerance of 5 kDa against the Consortium for Functional Glycomics database (www.functionalglycomics.org).

RESULTS

TIMP-1 Is a Target Protein for GnT-V in Colon Cancer Cells—GnT-V is an enzyme that catalyzes the attachment of a β1,6-GlcNAc linkage to the core *N*-linked glycan (Fig. 1*A*). We have identified target proteins for GnT-V from secreted glycoproteins that bind to lens culinaris column (13). However, glycoproteins did not necessarily bind to the lectin column, which prompted us to search for target proteins in this study from total secretome of WiDr:mock cells that expresses GnT-V at very low, almost negligible levels and GnT-V overexpressing cells (WiDr:GnT-V) (Fig. 1*B*). We performed comparative two-dimensional electrophoresis and lectin blot analyses of the secreted proteins using L_4-phytohemagglutinin (L-PHA), a lectin that basically recognizes the β1,6-GlcNAc moiety (Fig. 1*C*). Spots displayed differentially between WiDr:mock and WiDr:GnT-V were sliced, tryptic-digested, and identified by mass spectrometry. Fig. 1*C* shows a representative result of several independent experiments. Some proteins from WiDr:mock cells contain a β1,6-GlcNAc linkage in

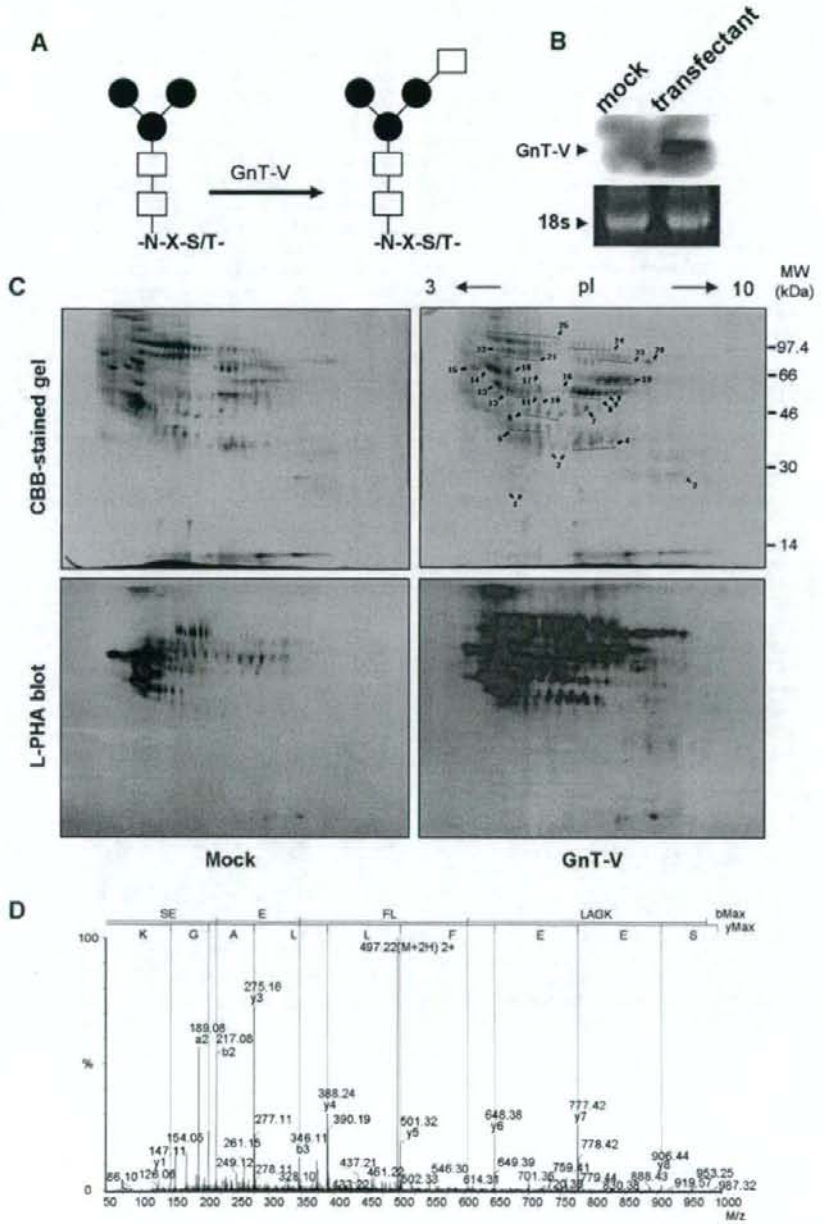

FIG. 1. **Search for target proteins of GnT-V in colon cancer WiDr cells and the identification of TIMP-1 as a candidate.** *A*, GnT-V-catalyzed addition of β1,6-GlcNAc to the core *N*-glycan comprised of GlcNAc (□) and mannose (●). *N*, asparagine; *S*, serine; *T*, threonine; *x*, any amino acid except proline. *B*, WiDr colon cancer cells were transfected with the *MGAT5* gene, and the stable transfectant cells were established. *C*, protein samples prepared by precipitation of WiDr conditioned serum-free media were displayed on two-dimensional electrophoresis gel. *Spots* that displayed differentially between WiDr:mock and WiDr:GnT-V cells were used for identification. Proteins indicated by *arrows* were identified as follows; *1*, heparan sulfate proteoglycan perlecan; *2*, tissue inhibitor of metalloprotease-1; *3*,

TABLE I

Proteins differentially recognized by L-PHA on 2-DE gels and identified by ESI-MS spectrometry and a Mascot blast search against NCBInr

Accession gi no.	Identities	Peptides matched	Sequence coverage (%)	Total score[a]	M_r/pI[b]	Levels[c] (±S.D.)
177836	α-1-antitrypsin precursor	7	26.3	438	46.7/5.5	0.26 (0.03)
15079348	Angiotensinogen preproprotein	3	10.1	189	53.1/5.8	1.19 (0.07)
4261632	β-N-acetylhexosaminidase A	10	22.3	575	60.7/5.0	1.77 (0.17)
54697170	Cathepsin D preproprotein	5	11.7	320	44.5/6.1	3.87 (0.24)
3650498	Cathepsin X precursor	2	5.9	107	33.9/7.1	1.19 (0.11)
68533097	DDR1 variant protein	3	4.4	141	99.0/6.3	0.66 (0.06)
16877430	Dipeptidyl peptidase 7 preproprotein	3	11.3	146	54.3/5.9	2.33 (0.17)
38327632	Discoidin receptor tyrosine kinase	2	6.1	99	96.9/6.1	1.40 (0.12)
4758116	Dystroglycan 1 precursor	2	3.3	106	97.6/8.7	1.42 (0.15)
5031863	Galectin 3 binding protein	3	6.8	147	65.3/5.1	0.53 (0.06)
4504151	Granulin isoform 1 precursor	3	5.7	149	63.5/6.4	1.21 (0.09)
5729877	Heat shock 70 kDa protein 8 isoform 1	7	14.6	379	70.9/5.4	2.47 (0.15)
15010550	Heat shock protein gp96 precursor	9	12.0	484	90.2/4.7	0.34 (0.04)
11602963	Heparan sulfate proteoglycan perlecan	3	1.1	171	466.6/6.0	3.26 (0.33)
16924217	Hexosaminidase B preproprotein	5	10.4	266	63.1/6.3	0.87 (0.06)
5080756	Human Fc binding protein	3	1.6	179	572.1/5.1	0.19 (0.02)
106586	Ig kappa chain V-III	3	25.1	252	23.1/5.8	1.48 (0.11)
9845498	Laminin γ1 precursor	11	8.7	746	177.6/5.0	1.47 (0.06)
56682964	Legumain preproprotein	3	12.7	152	49.4/6.1	1.54 (0.11)
51095116	Met proto-oncogene	7	5.3	471	155.4/7.0	1.76 (0.04)
4503899	N-acetylgalactosamine-6-sulfatase	5	14.9	295	58.0/6.3	0.63 (0.06)
4504061	N-acetylglucosamine-6-sulfatase	8	17.9	457	62.0/8.6	0.18 (0.02)
57209715	Prosaposin	5	10.9	318	58.1/5.1	2.01 (0.08)
4505989	Protective protein for β-galactosidase	2	5.4	178	54.5/6.2	0.35 (0.04)
2136061	Protein-tyrosine kinase-related receptor PTK7	7	9.2	432	118.3/6.7	0.47 (0.02)
57160745	Protein tyrosine phosphatase kappa	7	7.8	374	162.0/5.6	2.04 (0.07)
5231228	Ribonuclease T2 precursor	5	25.3	262	29.5/6.7	0.86 (0.07)
57210053	Tissue inhibitor of metalloproteinase-1	4	26.1	215	23.2/8.5	1.97 (0.06)
120749	Tumor-associated calcium signal transducer 1	2	11.8	184	34.9/7.4	1.08 (0.09)
38026	Zn-α-2-glycoprotein	4	19.5	234	34.7/5.7	0.41 (0.05)

[a]Total score is a sum of the score values obtained from each of an individual peptide. Score is −10 x Log (P), where P is the probability that the observed match is a random event; it is based on NCBInr database using the MASCOT searching program as MS/MS data.

[b]Molecular weight (M_r) and isoelectric point (pI) are theoretical values where glycan residues were not considered for the calculations. The theoretical values are prone to be changed by an attachment of glycans to peptides and thus to be different from the experimental values estimated on two-dimensional electrophoresis gels.

[c]Numbers refer to the relative levels of each protein from WiDr:GnT-V compared to those from WiDr:mock (n = 5).

N-linked glycans, suggesting that the β1,6-GlcNAc linkage on the protein molecules was acquired during cancer development of a normal cell, or the linkage is a cognate component in itself that is essential for either functional or structural integrity. In contrast, proteins from WiDr:GnT-V were more reactive to L-PHA compared with those from WiDr:mock. This may arise from a net increase in the β1,6-GlcNAc glycan moiety without any significant change in expression level, from simply the up-regulation of otherwise undetectable glycoproteins with a cognate β1,6-GlcNAc linkage, or from simultaneous increases in the β1,6-GlcNAc glycan moiety and protein levels. The identified proteins in several sets of independent experiments are compiled in Table I. To minimize the possibility of systematic errors, the proteins that were exactly matched to at least two unique peptides with significant score values ($p < 0.05$) and no miss were screened. Some proteins showed multispots, which is a common feature of some glycoproteins, and in this case, the lowest score values are

ribonuclease T2 precursor; *4*, cathepsin X precursor; *5*, Zn-α-2-glycoprotein; *6*, cathepsin D preproprotein; *7*, protective protein for β-galactosidase; *8*, legumain preproprotein; *9*, human Fc binding protein; *10*, discoidin receptor tyrosine kinase; *11*, angiotensinogen preproprotein; *12*, α-1-antitrypsin precursor; *13*, β-N-acetylhexosaminidase A; *14*, prosaposin; *15*, galectin 3 binding protein; *16*, *N*-acetylgalactosamine-6-sulfatase; *17*, dipeptidyl peptidase 7 preproprotein; *18*, heat shock 70 kDa protein 8 isoform 1; *19*, hexosaminidase B preproprotein; *20*, granulin isoform 1 precursor; *21*, *N*-acetyl-glucosamine-6-sulfatase; *22*, heat shock protein gp96 precursor; *23*, DDR1 variant protein; *24*, protein-tyrosine kinase-related receptor PTK7; *25*, protein tyrosine phosphatase κ. *D*, peptide derived from *spot 2* in *panel C* was sequence analyzed by ESI/Q-TOF mass spectrometry, blasted against the Mascot database, and identified to be human TIMP-1 from the sequence SEEFLIAGK seen in the mass spectrum together with other sequences.

shown in Table I. All the proteins in Table I were confirmed by an independent, the more direct approach: protein samples were reduced by β-mercaptoethanol to minimize the possibility of "junk proteins" interacting with the glycoproteins and were thereafter subject to desalting to remove β-mercaptoethanol. Precleared with avidin-agarose beads, the reduced proteins were allowed to interact with L-PHA-avidin-agarose beads. After intensive washing, the bound proteins were completely denatured in an SDS-PAGE denaturation buffer, resolved on a minimal size of SDS-PAGE gels, and digested in gel by trypsin. The tryptic peptides were eluted out and sequence analyzed with an LTQ-FTICR (7 Tesla) mass spectrometer equipped with a nanoelectrospray ion source. Blast search was carried out as described in "Experimental Procedures." The identified proteins that derived from WiDr:GnT-V but not WiDr:mock and the related information are available in supplemental Fig. 1. Fig. 1*D* shows a representative peptide sequence of TIMP-1 as determined by ESI/Q-TOF and a Mascot blast search program.

Changes in the serum level of proteins associated with diseases are of great interest in biomarker discovery, and glycoproteins constitute a significant portion of serum proteins. In this regard, the levels of proteins in the WiDr-conditioned RPMI 1640 media were also investigated using the differential in-gel electrophoresis method. Proteins from WiDr:mock and WiDr:GnT-V were labeled with cy3- and cy5-fluorescent dyes, respectively, resolved on two-dimensional gels, and the fluorescent intensities of each spot were measured. supplemental Fig. 2 shows a representative result of five independent experiments. Some of the glycoproteins show multispots on a two-dimensional electrophoresis gel, and even a glycoprotein of the same protein identity were not overlapped at least in our case, where the glycan changes result in a shift in migration on a gel. Thus, each spot was reidentified by mass analysis after quantification. As noted in Table I, many of the proteins show an increased level in GnT-V overexpressing cells, while some proteins were either decreased or did not show any dramatic alteration. Both changes in glycan structure and the altered levels of the proteins, as described in Table I, could provide an important clue for further study in which the candidate proteins could be validated in human blood or proximal biofluids.

TIMP-1 is an endogenous inhibitor of MMPs that play a critical role in cancer cell invasion and migration and has been reported to be implicated in the malignant transformation of cancer cells in some manner (18). For this reason, TIMP-1 was chosen as a model glycoprotein to show how an aberrant glycosylation induced by GnT-V affects cancer progressions and malignancy, and it was hypothesized that, at least in part, the pathological symptoms manifested by the action of GnT-V result from an alteration in the *N*-glycan structure of TIMP-1.

Establishment of Stable Transfectants of TIMP-1 and the Glycosylation Mutants—To examine the effects of GnT-V-initiated alterations of *N*-linked glycans on TIMP-1 on cancer cell behavior, site-directed mutageneses were performed in which either or both of Asn^{30} and Asn^{78} were replaced with Gln (Fig. 2*A*). Together with the wild-type *TIMP-1* gene, the three mutated genes were transfected into cells and designated as T-N30Q, T-N78Q, and T-N30/78Q. The repetitive transfections and selections were conducted so as to meet two requirements: the first is that the amounts of TIMP-1 recombinant protein (rTIMP-1) secreted are as much as possible so as to minimize the effects of cognate TIMP-1. The other is that the amounts of rTIMP-1 proteins secreted are equal among the transfectants in order to exclude the differences in cancer cell behavior arising from difference in the levels of secreted TIMP-1. Stable transfectants satisfying both requirements were selected based on an immunoblot analysis (Fig. 2*B*). The secretion level of cognate TIMP-1 was 18.4 ± 0.8% of that for rTIMP-1 in WiDr:GnT-V cells and negligible in case of WiDr:mock cells as assessed by using Quantity One software program (Bio-Rad). The molecular mass of the mature form of TIMP-1 is ~28.5 kDa, of which *N*-linked glycans account for about 8 kDa (19). The eradication of either of the two *N*-linked glycosylations produced rTIMP-1 mutant proteins whose molecular masses were reduced by 4 kDa, confirming that the intended transfectant cells were produced.

To deduce the structure of aberrant glycan of TIMP-1, the cognate TIMP-1 was purified both from WiDr:mock and WiDr:GnT-V and subjected to two-dimensional electrophoresis followed by immunoblot using an anti-TIMP-1 antibody or a lectin blot analysis using L-PHA and *Datura stramonium* agglutinin (DSA), a lectin recognizing lactosamine moiety (Fig. 2*C*). TIMP-1 from WiDr:mock was divided into one main spot in the basic region and two minor ones in the acidic region on two-dimensional electrophoresis gels, indicating that only small fraction of TIMP-1 possibly carries an acidic glycosyl residue such as sialic acid. None of the subdivisions carried β1,6-GlcNAc or lactosamine linkages. However, the majority of the aberrant TIMP-1 showed β1,6-GlcNAc linkages and extended polylactosamine glycan moieties. Moreover, TIMP-1 was divided into multispots on two-dimensional electrophoresis gels, showing an increment of heterogeneity. Taken together, TIMP-1 aberration is characterized by the attachment of β1,6-GlcNAc linkages, polylactosaminylation, and an increase in terminal elaborations with acidic residue. Besides, it appears that the secretion level of TIMP-1 is elevated upon the attachment of aberrant *N*-glycan (Fig. 2*B*).

Mass analysis of *N*-glycans of TIMP-1 was performed on a MALDI-TOF mass spectrometer (Fig. 3*A*). The *N*-glycan structures were deduced from the *m/z* values of the detected ions, which were blasted against the Consortium for Functional Glycomics database, and the most relevant composition of the monosaccharide building blocks were assigned. The heterogeneous *N*-glycans of TIMP-1 from WiDr:mock were resolved in the range of 1500–3500 *m/z*, all of which were deviated from the calculated value (~4 kDa), consistent with the previous measurement (20). Overall, the average mass of

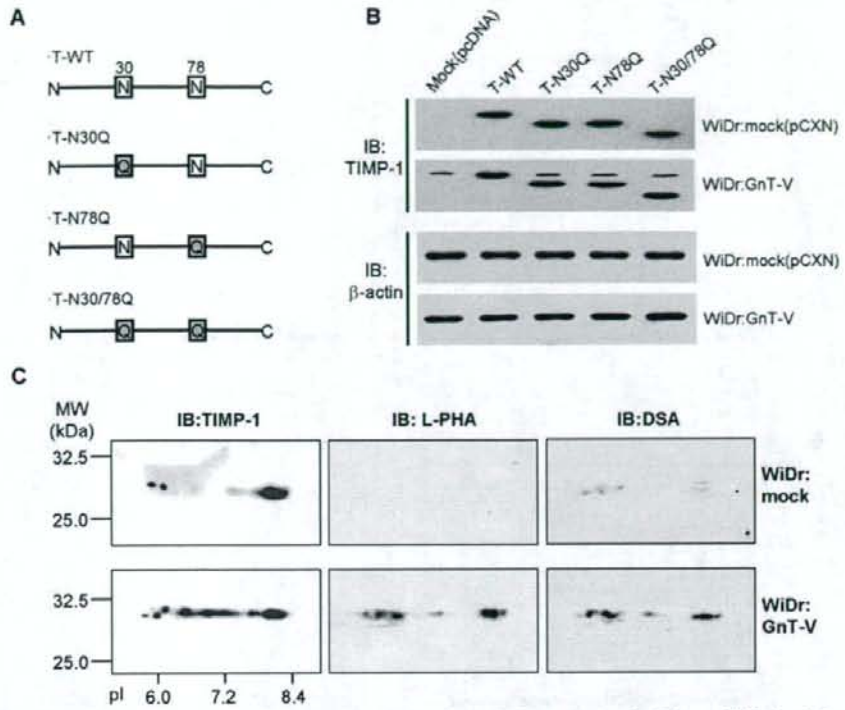

FIG. 2. **Establishment of stable transfectants of TIMP-1 and the glycosylation mutants.** *A*, wild-type *TIMP-1* and three glycosylation mutant genes were cloned. *B*, the cloned genes were transfected into WiDr:mock and WiDr:GnT-V cells, and the stable transfectants expressing equal amounts of the recombinant proteins were selected. *C*, the structure of the aberrant glycan on TIMP-1, initiated by the GnT-V-catalyzed attachment of β1,6-GlcNAc, was deduced by two-dimensional electrophoresis combined with lectin and immunoblot (*IB*) analyses. β1,6-GlcNAc and additional polylactosamine moieties could be deduced from the L-PHA and DSA blot, respectively, in aberrant TIMP-1 molecules. *MW*, molecular mass.

N-glycans of TIMP-1 from WiDr:GnT-V was higher than that from WiDr:mock, and the GnT-V-catalyzed TIMP-1 showed the more heterogeneous profiling of *N*-glycans. Interestingly, the masses of some *N*-glycans of TIMP-1 from WiDr:GnT-V were calculated to differ by ~1035 *m/z*. That is, mass values of peaks at 1809, 2421, and 3353 *m/z* in WiDr:mock match those peaks at 2847, 3458, and 4388 *m/z*, respectively, when the increment value is subtracted. Considering an increment in mass during esterification of *N*-acetylneuraminic acid (Neu), the increment value corresponds to the molecular mass of adducts, $Neu_1Gal_2GlcNAc_2$. Upon *N*-acetylglucosaminylation, galactose (Gal) and GlcNAc were alternatively added, and terminal Neu was then decorated. It is, however, not clear whether the glycan of 4127 *m/z*, marked with asterisk (*), was derived from that of 2785 *m/z* by gaining another sialic acid or if it was derived from another glycan substrate, possibly ~3092 *m/z*, and the glycan of 3092 *m/z* was not detected in the profiling of *N*-glycans from WiDr:mock. Two repeats of lactosamine residues on the adducts are thought to confer reactivity toward the DSA lectin, and Neu residues produce the heterogeneous behaviors on two-dimensional electrophoresis gels. Indeed, *N*-glycans from WiDr:mock are neutral or contain 2 Neu residues, whereas those from WiDr:GnT-V have various numbers (0–4) of Neu residues. The composition of the annotated glycans in Fig. 3*A* was confirmed by a mass analysis of each glycan that had been treated with sialidase (Fig. 3*B*) and sialidase plus β-galactosidase (Fig. 3*C*). For example, the glycan with *m/z* 2785 from WiDr:mock was estimated to be reduced to $Gal_3Man_3GlcNAc_5Fuc_1$ (*m/z* 2176) by the loss of two residues of Neu when treated with sialidase, which were, in turn, further processed to $Man_3GlcNAc_5Fuc_1$ (*m/z* 1690) by treatment with β-galactosidase and sialidase.

Effects of the Aberrant Glycosylation of TIMP-1 on In Vitro Cell Migration and Invasion—Cumulative studies indicating that an increase in GnT-V activity correlates with the high invasive/metastatic potential of cancer cells and the fact that TIMP-1 is associated with the potential prompted us to examine the role of *N*-linked glycosylation of TIMP-1 in the metastatic potential of colon cancer cell. For this, the migra-

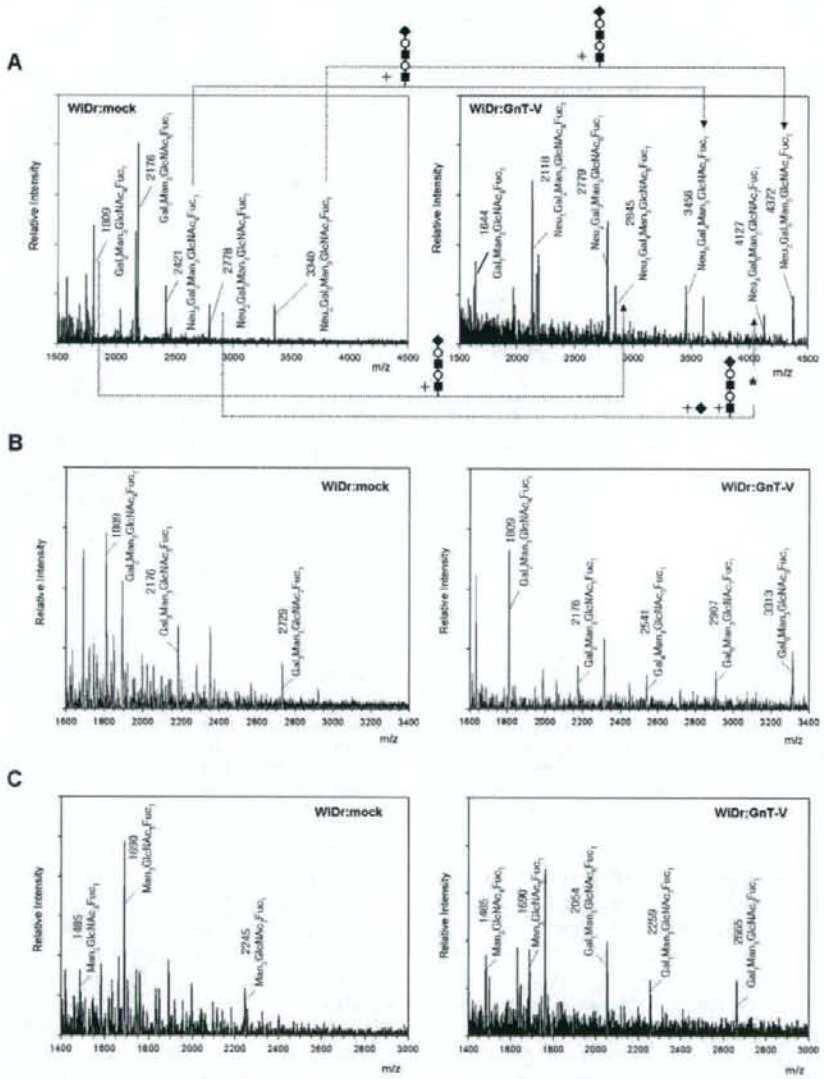

FIG. 3. **Profiling of *N*-glycans of TIMP-1 in WiDr cells.** *A*, profiling of TIMP-1 glycans from WiDr:mock and WiDr:GnT-V was performed. Glycans digested with PNGase F were mass analyzed in a MALDI-TOF mass spectrometer, and the composition of each glycan was deduced from the mass value. The annotated composition was confirmed by treatment with sialidase (*B*) and β-galactosidase plus sialidase (*C*). ■, *N*-acetylglucosamine; ○, galactose; ♦, *N*-acetylneuraminic acid.

tion and invasion properties of each TIMP-1 transfectant were investigated *in vitro*. Concerning cell migration, GnT-V affected cell migration, but in a TIMP-1-independent manner (Fig. 4*A*). Little difference in the motility was observed among the TIMP-1 transfectants of WiDr:mock cells as well as WiDr:GnT-V cells. However, GnT-V conferred a higher motility on WiDr cells irrespective of the mutational status of TIMP-1, indicating that the increment of cell motility is actually aided by GnT-V but possibly mediated by other mediator proteins or through a signal transduction pathway independent of TIMP-1 as reported previously (6).

Meanwhile, glycan moieties on TIMP-1 affected the cell invasion significantly (Fig. 4*B*). T-N30/78Q:GnT-V cells showed a dramatically slow cell invasion compared with T-WT:GnT-V,